260

N_2/SF_6 MIXTURES FOR GAS INSULATED SYSTEMS

Task Force D1.03.10

October 2004

cigré

N_2/SF_6 MIXTURES FOR GAS INSULATED SYSTEMS

TASK FORCE D1.03.10

Members:

W. Boeck (Convener), T.R. Blackburn, A.H. Cookson, A. Diessner, F. Dorier, F. Endo, M. Ermel, K. Feser, A. Giboulet, A. Girodet, S. Halliday, B.F. Hampton, W. Koltunowicz, H.-G. Kranz, J. Lopez-Roldan, L. Lundgaard, Li Ming, S. Meijer, C. Neumann, R. Pietsch, U. Riechert, W. Rutgers, U. Schichler, H. Slowikowska

SUMMARY

N_2/SF_6 gas mixtures possess good insulation properties, even at low SF_6 contents. Adequate dielectric properties can be achieved with SF_6 contents of 10 to 20%, which are regarded as reasonable for GIL applications when technical, economic and environmental aspects are considered. Only a modest pressure increase of about 45 to 70% is necessary to recover the dielectric strength of pure SF_6, and the amount of SF_6 required, and the SF_6 leakage rate, will be considerably reduced by approximately 70 to 85%. The influence of field enhancements caused by electrode curvatures and surface roughness can easily be taken into account for the design of the equipment.

The breakdown voltage in the presence of defects in such mixtures is slightly lower than in pure SF_6 of equal dielectric strength. However, all existing diagnostic systems can be applied in these mixtures, with an equivalent or higher detection sensitivity than in pure SF_6. The discharge current and signal emission of fixed defects at live parts are similar to those in pure SF_6. The signal emission from mobile particles is independent of the gas type and mixture ratio. All methods for defect diagnosis can be applied in the same way as for SF_6 insulation in GIS.

The heat transfer capability and cooling properties are similar for SF_6 and N_2/SF_6 mixtures of equal dielectric strength. Such mixtures therefore permit the same power transfer capability for a GIL as pure SF_6. The pressure increase by an internal arc is higher than in pure SF_6, but in GIL there are usually large gas volumes which restrict the overpressure. The resulting roots of internal arcs are much smoother than in pure SF_6.

The arc quenching ability at current zero, and the resulting current interruption performance in such mixtures, is poor. Even the switching capability of disconnectors for small bus charging currents is considerably degraded. The leader channel changes its direction more often, and there is a much higher risk for leader branching and flashover to ground during arcing between contacts in such mixtures than in SF_6. Therefore these mixtures are not suitable for any switching duties. The total reduction in SF_6 used in a partially N_2/SF_6 insulated GIS where all compartments with switching devices are filled with pure SF_6 would be minimal. In GIS, therefore, the substitution of SF_6 by N_2/SF_6 mixtures would lead to uneconomical technical solutions and would have no ecological advantage.

1. INTRODUCTION

SF_6 is used in power apparatus as an insulating and arc quenching medium because of its excellent insulating and arc extinguishing properties. However, its global warming potential has prompted discussion on replacing SF_6 in power equipment. Therefore SF_6 substitutes such as N_2/SF_6 mixtures are undergoing thorough investigations in which their dielectric performance under clean conditions, as well as with defects and the switching performance, are of most interest. The scope of this brochure is restricted to high voltage switchgear and power transmission systems. A distinction must be made between applications of N_2/SF_6-gas mixtures in Gas Insulated Lines (GIL), Gas Insulated Switchgear (GIS) and Circuit-Breakers (CB).
This brochure focuses on the necessary fundamentals and data for the application of N_2/SF_6 mixtures in insulation systems of electrical power equipment. A short version has been published in a CIGRE Report [1]. In CIGRE Brochure 163 [2] further important aspects of N_2/SF_6 mixtures are mainly considered. N_2/SF_6-mixtures are applied in hardly anything but the GIL technology, which is treated in CIGRE brochure 218 [3].

2. BASIC DISCHARGE PROPERTIES

At low SF_6 concentrations N_2/SF_6 mixtures have high dielectric strengths due to the unique synergetic properties of their components. Therefore N_2/SF_6 mixtures can be applied which, like natural air, consist mainly of nitrogen. Natural N_2 is chemically even more inert than SF_6, but less expensive. It causes fewer decomposition products during arcing e.g., during switching operations and faults, and its emission into the atmosphere by leakages and further gas losses has no environmental impact at all.

Most essential for gas insulated systems is the dielectric strength of these mixtures. The intrinsic dielectric strength of the gas mixture, not affected by roughness or defects at surfaces of ambient solid material, is the main basis for the choice of the mixture ratio, the gas pressure and the design of the insulation system. Under such ideal conditions its characteristics can be derived from the gas discharge process. The effective ionisation coefficient $\bar{\alpha}$ governs the electron multiplication and discharge development. It takes into account ionisation and attachment processes. Both components contribute to the effective ionisation coefficient of the mixture through their individual effective ionisation coefficients ($\bar{\alpha}_{SF6}$, $\bar{\alpha}_{N2}$), according to the SF_6 content x and the N_2 content $(1 - x)$ in the mixture [4].

$$\bar{\alpha} = x\bar{\alpha}_{SF6}\left(\frac{E}{p}\right) + (1-x)\bar{\alpha}_{N2}\left(\frac{E}{p}\right) \qquad (1)$$

Fig. 1 presents the pressure reduced effective ionisation coefficients $\bar{\alpha}/p$ over the pressure reduced field E/p for pure SF_6 and N_2. These ionisation characteristics are usually approximated by a linear function for SF_6

$$\frac{\bar{\alpha}_{SF6}}{p} = k_{SF6}\left(\frac{E}{p} - \left(\frac{E}{p}\right)_{crSF6}\right) \quad (2a)$$

and by a non-linear function for N_2

$$\frac{\bar{\alpha}_{N2}}{p} = A\exp\left(-\frac{B}{E/p}\right) \qquad (2b)$$

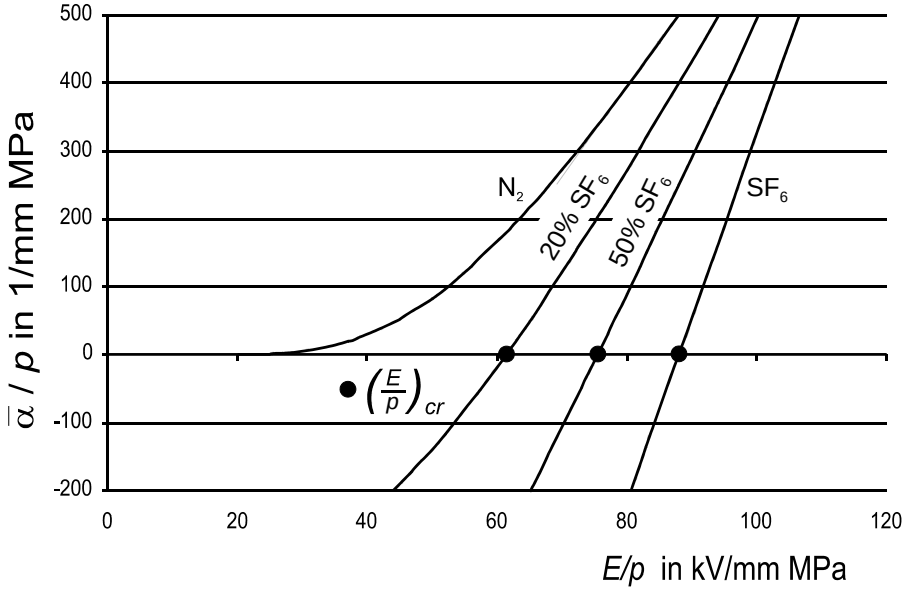

Fig. 1: *Pressure reduced effective ionisation coefficient $\bar{\alpha}$ for N_2/SF_6 mixtures, pure SF_6 and pure N_2.*

Insignificantly varying parameters k_{SF6}, $(E/p)_{crSF6}$, A and B are applied in literature. Standard values are chosen and proposed for common application [5]:

$$k_{SF6} = 27\,\frac{1}{\mathrm{kV}} \qquad \left(\frac{E}{p}\right)_{crSF6} = 87{,}8\,\frac{\mathrm{kV}}{\mathrm{mm\,MPa}}$$
$$A = 6600\,\frac{1}{\mathrm{mm\,MPa}} \qquad B = 215\,\frac{\mathrm{kV}}{\mathrm{mm\,MPa}} \qquad \text{(2c)}$$

For N_2/SF_6 mixtures of practical interest (SF_6 content ≥ 10%) the ionisation characteristics (Fig. 1) obtained by Equ.(1) and (2) become approximately linear functions:

$$\frac{\bar{\alpha}}{p} = k\left(\frac{E}{p} - \left(\frac{E}{p}\right)_{cr}\right) \qquad (3)$$

The parameters k and $(E/p)_{cr}$ are listed in Table 1.

Electron multiplication can happen only in the critical volume where $\bar{\alpha} \geq 0$ and $(E/p)_{cr}$ are exceeded. If there is an initial seed electron and a sufficient electron multiplication, a streamer discharge will be launched which either causes partial discharges or direct breakdown. Seed electrons emerge randomly, and cause a statistical scatter of streamer inception. The minimum streamer inception voltage can be calculated by the criterion

$$\int_0^{l_{cr}} \bar{\alpha}\, dl = K \qquad (4)$$

The integration has to be performed in the critical volume (Fig. 2) along the line of force from the point $l = 0$ of maximum field stress E_{mi} to $l_{cr,}$ where the field reaches the critical value:

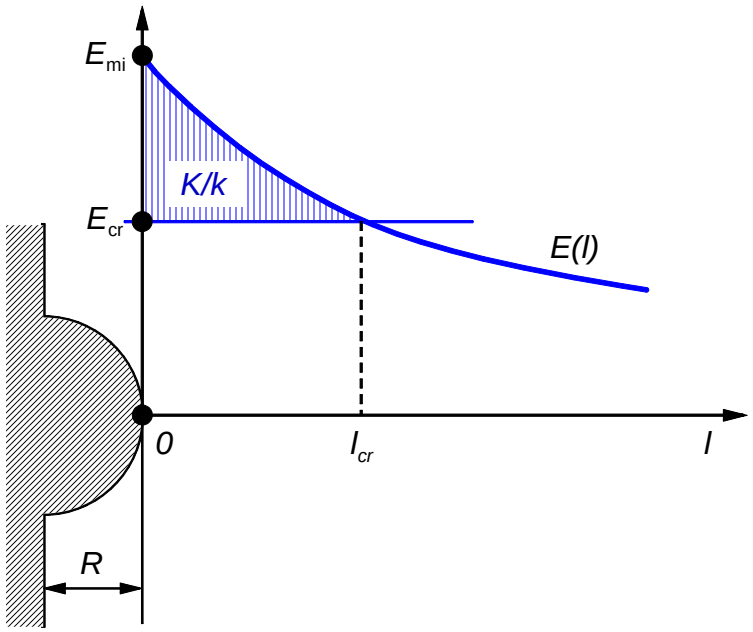

Fig. 2: *Field distribution for streamer inception at the minimum streamer inception voltage U_i.*

Table 1: *Basic parameters for N_2/SF_6 mixtures and pure SF_6 (M see chapter 5.1)*

x	$\left(\frac{E}{P}\right)_{cr}$ [5]	k [5]	K	K/k	M
	$\frac{\text{kV}}{\text{mm MPa}}$	1/kV		kV	µm MPa
1,0	87,8	27,0	10,5	0,389	4,43
0,9	85,5	25,9	9,95	0,384	4,49
0,8	83,1	24,7	9,40	0,381	4,59
0,7	80,5	23,4	8,85	0,378	4,70
0,6	77,6	22,5	8,30	0,369	4,76
0,5	74,2	21,2	7,75	0,366	4,93
0,4	70,4	19,8	7,20	0,364	5,17
0,3	65,9	18,2	6,65	0,365	5,54
0,2	60,2	16,0	6,10	0,381	6,33
0,1	52,1	12,6	5,55	0,440	8,45

$$E(l_{cr}) = E_{cr} = p\left(E/p\right)_{cr} \qquad (5)$$

The streamer parameters K for SF_6 and N_2 in Equ. (4) are taken from breakdown data of Cigre [5,6]:

$$\text{SF}_6 : K_{SF6} = 10,5 \qquad \text{N}_2 : K_{N2} = 5 \qquad (6)$$

The streamer parameters K for N_2/SF_6 mixtures in Table 1 are gained by linear interpolation according to the individual content of both gas components [7]

$$K = K_{SF6}x + K_{N2}\left(1-x\right) \qquad (7)$$

In inhomogeneous fields, as shown in Fig. 2 ahead of a curved electrode, streamer discharge inception will occur according to the criterion based on Equ. (4) and (3)

$$\int_0^{l_{cr}} \left(E(l) - E_{cr} \right) dl = K / k \qquad (8)$$

when the hatched voltage area in Fig. 2 has the value K/k, which is listed in Table 1 and found to be almost constant for all N_2/SF_6 mixtures of interest in practice [7]:

$$K / k = 0{,}380 \text{ kV} \qquad (9)$$

The maximum field E_{mi} at streamer inception and the corresponding streamer inception voltage U_i will exceed the critical field E_{cr} and the corresponding critical voltage U_{cr} respectively. However in slightly inhomogeneous fields of sound insulated systems, streamer inception at E_{mi} and U_i occurs near E_{cr} and $U_{cr;}$ whereas in strongly inhomogeneous fields at defects it will occur considerably above E_{cr} and U_{cr}. Since there are no discharges below streamer inception and all discharge phenomena until breakdown are initiated by streamers (Chapter 4), E_{mi} and U_i normally stand for discharge inception.

The intrinsic dielectric properties of the gas mixture are valid under the ideal conditions of a strictly homogeneous DC field between perfectly smooth electrode surfaces. In such a field with a gap length d, streamer inception occurs when the constant field E_i exceeds the critical field $E_{cr} = \left(E / p \right)_{cr} p$ over the whole gap according to

$$\int_0^{d} \left(E_i - E_{cr} \right) dl = K / k \qquad (10)$$

and the minimum streamer inception field E_i and voltage U_i becomes

$$U_i = E_i d = (E / p)_{cr} \, p \, d + K / k \qquad (11)$$

In the case of DC stress breakdown occurs at U_i, and Equ. (11) corresponds with the Paschen curve as found experimentally at low pressures where the results are not affected by surface roughness [7]. The breakdown value exceeds the critical voltage $U_{cr} = (E/p)_{cr} \, pd$ by the minimum voltage of the Paschen curve K/k. In high voltage equipment this small value can be neglected. The critical field $E_{cr} = (E/p)_{cr} \cdot p$ can therefore be regarded as the intrinsic dielectric strength of the gas mixture.

3. ADVANTAGES AND PREFERENTIAL APPLICATION

The intrinsic dielectric strength E_{cr} of the mixture relates to its strength under ideal conditions, but can be applied for quite accurate estimations of practical properties when normalized values are used. Fig. 3 shows the normalized intrinsic dielectric strength $E_{cr}^0 = \left(E / p \right)_{cr} / \left(E / p \right)_{cr\,SF6}$ from Table1 for N_2/SF_6 mixtures as function of the SF_6 content x. It permits quantitative analysis of the essential properties and advantages of N_2/SF_6 mixtures, and provides a basis for many fundamental considerations. Even mixtures with low SF_6 content are seen to exhibit a high dielectric strength. For example, a mixture with only 20% SF_6 content has 69% of the dielectric strength of pure SF_6 at an equal gas pressure.

When determining the optimum SF_6 content, mixtures of equal intrinsic dielectric strength E_{cr} have to be considered. The normalized pressure p^0 of such mixtures, $p^0 = 1/E^0_{cr}$, is also presented in Fig 3. In the example containing 20% SF_6, a modest pressure increase of about 45% is necessary to achieve the dielectric strength of pure SF_6. Furthermore, it is important to consider the total amount of SF_6 required for a given application. This can be seen in Fig. 3 as the normalized quantity $q^0 = x\,p^0$ of SF_6 in mixtures of equal intrinsic dielectric strength. A mixture containing 20% SF_6 reduces the required amount of SF_6 by 71% compared with pure SF_6 of equal dielectric strength. SF_6 leakage is also governed by the quantity q^0 when mixtures are applied in electrical equipment of the same design, material and quality. The leakage would also be reduced by 71% in the example considered.

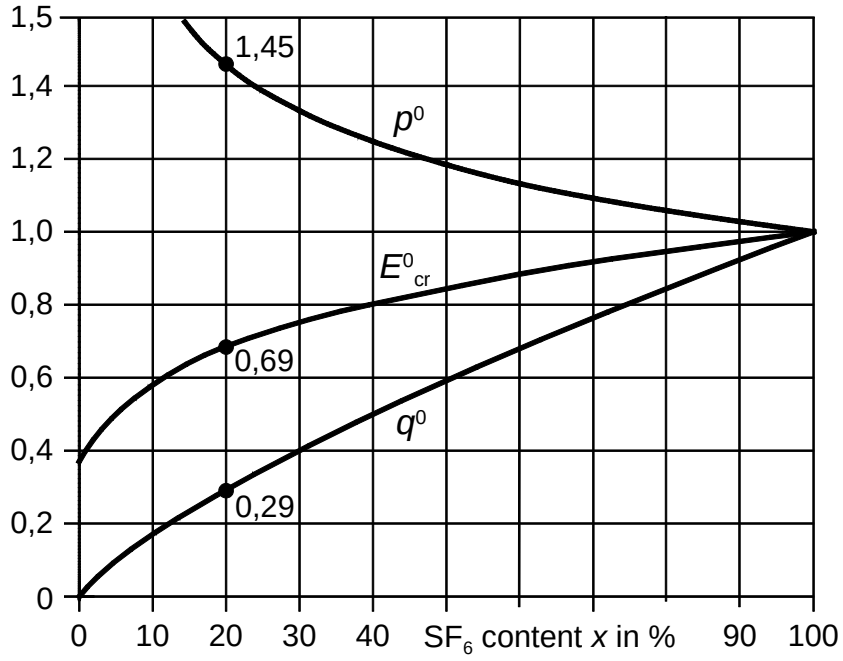

Fig. 3: *Normalized intrinsic dielectric strength E^o_{cr}, normalized pressure p^0 required for equal dielectric strength and resulting normalized quantity q^0 of SF_6 as a function of the SF_6 content x.*

In GIL, large amounts of insulating gases are needed. For example a 420 kV GIL, 10 km long and with a diameter of 600 mm, would require about 200 tonnes of pure SF_6 (about 20% of the total currently utilised in HV plant in Germany). An N_2/SF_6 mixture of 80%/20% with a pressure of 0,8 MPa would require about 58 tonnes of SF_6, only 29% of the pure SF_6 case. Furthermore, a considerable reduction in cost could be achieved using a gas mixture. Lowering the percentage of SF_6 could reduce the overall amount of SF_6 further, but may require the introduction of special pressure vessels, since the total gas pressure would have to rise accordingly.

Using pure N_2 would require a pressure of more than 1,5 MPa, even without considering further technical disadvantages such as the loss of corona stabilisation. This rather high pressure would necessitate a special construction for the enclosure, and this might conflict with the relevant pressure vessel regulations. Adequate dielectric properties can be achieved by N_2/SF_6-gas mixtures containing 10 to 20% SF_6, regarded as reasonable for GIL applications when technical, economic and environmental aspects are considered.

In GIS, SF_6 is used because of its excellent insulating and arc quenching properties, which enable a space-saving switchgear design. The poor arc quenching properties of N_2/SF_6 mixtures are an important consideration for GIS. Compartments containing switching equipment, in particular

circuit-breakers, but also disconnectors, need pure SF_6 for proper current interruption. Substituting pure SF_6 by an 80%/20% N_2/SF_6 mixture would decrease the switching capability considerably. Only in compartments where the SF_6 functions merely as an insulator could it be substituted by a N_2/SF_6 gas mixture. Depending on the specific GIS design, between 20 and 52% of the total amount of SF_6 is in compartments where it functions solely as an insulator (Fig. 4). On the basis of a N_2/SF_6 mixture ratio of 80%/20% at a pressure of 0,8 MPa, the reduction in SF_6 used would be between just 14 and 37%. The reduction in the total amount of SF_6 is therefore minimal. Any benefit would be offset by the rather complicated gas handling that would have to be introduced, risking further emissions and increasing costs. In GIS therefore, the substitution of SF_6 by N_2/SF_6 mixtures would lead to uneconomical technical solutions and would have no ecological advantage.

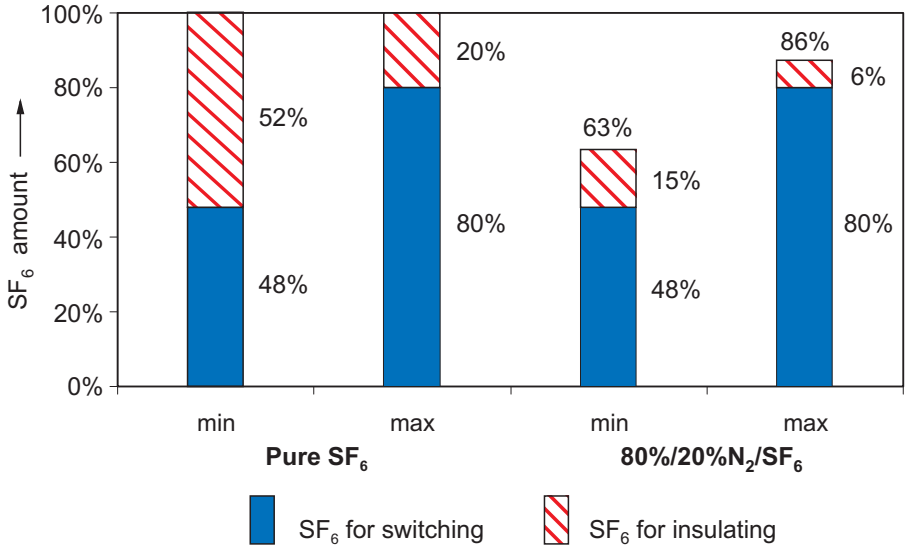

Fig.4: *Total amount of SF_6 in a specific GIS design with regard to switching and insulating functions, for pure SF_6 and its substitution by a 80%/20% N_2/SF_6 mixture [8].*

In outdoor circuit-breakers, SF_6 is used mainly as an arc quenching medium, but also performs an insulating function. Substituting SF_6 by a N_2/SF_6 mixture would introduce a requirement for additional switching units to obtain the same switching capability as before. Normally the number of interrupting units would have to be at least doubled when 50% N_2 content is used (this is necessary only for low temperature applications, when SF_6 liquefaction has to be avoided).

4. DISCHARGE DEVELOPMENT AND BREAKDOWN

In real insulation systems of electrical equipment the dielectric strength deviates from the intrinsic dielectric strength of gas mixtures for many reasons. The deviations are caused by the voltage waveform, the field distribution according to the design, the usual surface roughness of the electrodes and defects like mobile or fixed particles. The mechanism of the entire discharge development until breakdown is the same for all strongly electronegative N_2/SF_6 mixtures with an SF_6 content of more than (0,1 ... 1)% [9]. The complete discharge development [10] is explained by Fig. 5.

At streamer or discharge inception, the area A in Fig. 5 exceeds the critical value K/k. Then the critical volume V_{cr} becomes ionized, conducting and charged so that the internal field is reduced to almost $E_{cr,}$ and the remaining ionization balances the drain of ions and electrons due to their field drift. Within this initial streamer there is consequently a constant field E_{cr} and a corresponding

linearly falling potential Φ_s with the slope E_{cr}. This differs from the original background potential Φ and field E in the surrounding region. The resulting potential drop $\Delta\Phi$ at the edge of the initial streamer causes a restricted local field enhancement beyond E_{cr}, which is not shown in Fig. 5. At random locations having the most favourable conditions, the streamer continues to develop forward in filaments. Thus the streamer propagates further in filaments until the potential drop $\Delta\Phi$ becomes zero, the hatched areas A and B are equal and each of them has the value K/k. Since K/k is constant for all N_2/SF_6 mixtures the streamer size at streamer inception depends only on the critical field, and is therefore the same for N_2/SF_6 mixtures of equal intrinsic dielectric strength. The final streamer length l_s is limited. A streamer breakdown can occur only when l_S reaches the gap length between the electrodes, and the mean applied field exceeds the critical field.

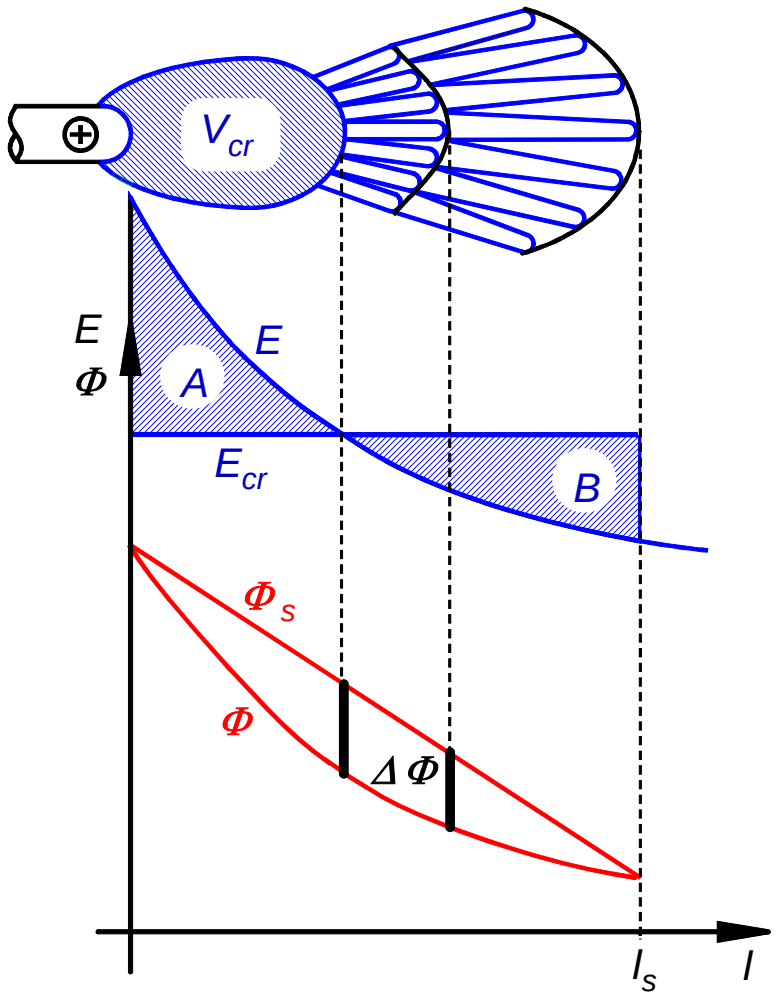

Fig. 5: *Streamer development in SF_6 with the internal (E_{cr}, Φ_s) and external original background (E, Φ) field and potential distribution.*

In normal insulation systems of electric power equipment, breakdown occurs at lower voltages due to additional leader development. The leader is launched at the tip A of a streamer filament and develops towards the electrode (Fig. 6). Due to its small voltage drop the developed leader acts like a protruded electrode. The first streamer (1) vanishes, and a new one (2) develops in the same manner at the leader tip, followed by a second leader. The streamer to leader transition at the first leader step results inevitably in breakdown, since the field at the leader tip is enhanced by each step. During this stepwise leader development to breakdown, leader branching sometimes occurs; e.g. at A, when by chance leader development is initiated simultaneously in more than one filament of a streamer, e.g. at B and C [Chapter 7].

Leader inception occurs when the charge of the ionized streamer attains a critical value [9]. The streamer charge grows with the gas pressure p and the streamer extension l_s. In the case of sound insulated systems with the usual electrode curvature and roughness, the streamer at the roughness peaks has a large extension (Fig. 7a). It causes at usual pressures immediate leader inception and breakdown, since the charge of the initial streamer exceeds the critical value for leader inception. The streamer inception criterion can be used to determine the breakdown voltage (chapter 5.1 and 5.2). However, in the strongly inhomogeneous field at defects there is a small streamer extension (Fig. 7b). For the usual pressures below a critical value, leader inception occurs at higher voltages and is decisive for breakdown (chapter 5.3). This allows PD measurements for defect diagnosis to be applied between both inception voltages (chapter 6).

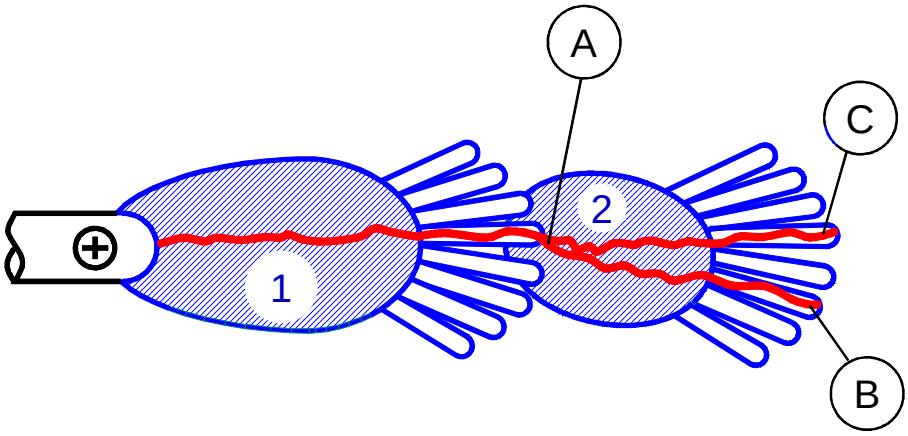

Fig. 6: *Two steps of leader development with the first (1) and the second (2) streamer.*

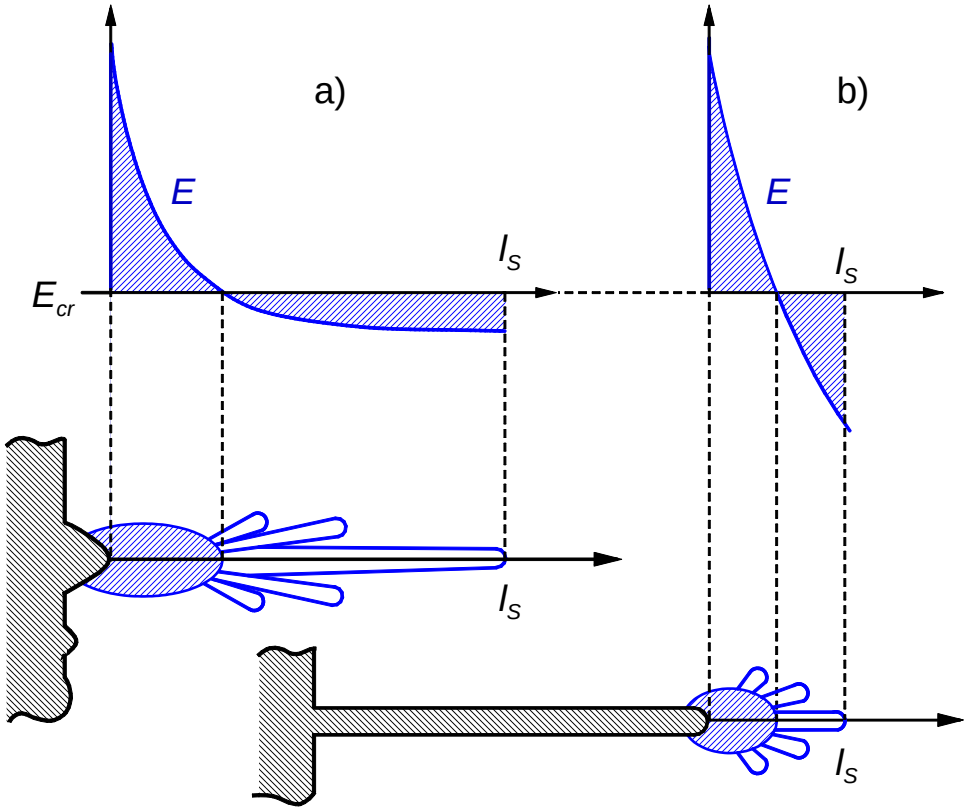

Fig. 7: *Field distribution and streamer extension at roughness peaks (a) and needle shaped defects (b).*

In the case of defects, the discharge inception and leader breakdown voltage may be additionally raised by corona stabilization, due to the space charge accumulation ahead of the streamer and the resulting field reduction. This happens when the ion drift velocity exceeds the velocity of the streamer growth, according to the extending critical volume during the voltage rise. This is predominantly given for AC and SI voltages, and defects with small tip radii causing especially high field inhomogeneities.

Especially in the case of steep impulse voltages such as LI, the statistical scatter and breakdown channel formation cause remarkably enhanced breakdown values. There are a few conditions which have to be met for breakdown to occur (Fig. 8). First, the minimum discharge inception voltage U_i has to be exceeded. Secondly, a seed electron is necessary in the critical volume where the critical field is exceeded, for initiation of the electron multiplication process. Due to the high attachment coefficient (η) such seed electrons are rare in electronegative gases. The production of the first seed electron occurs randomly and depends on $\bar{\alpha}/\alpha$, which was found to be approximately the same for N_2/SF_6 mixtures of equal dielectric strength [11]. The resulting statistical time lag t_s causes a scatter in the breakdown voltages for the case of lightning impulses. But the statistical distribution is similar for such mixtures. All testing procedures to verify the dielectric withstand level developed for SF_6 insulation can therefore also be applied for N_2/SF_6 insulated equipment [11].

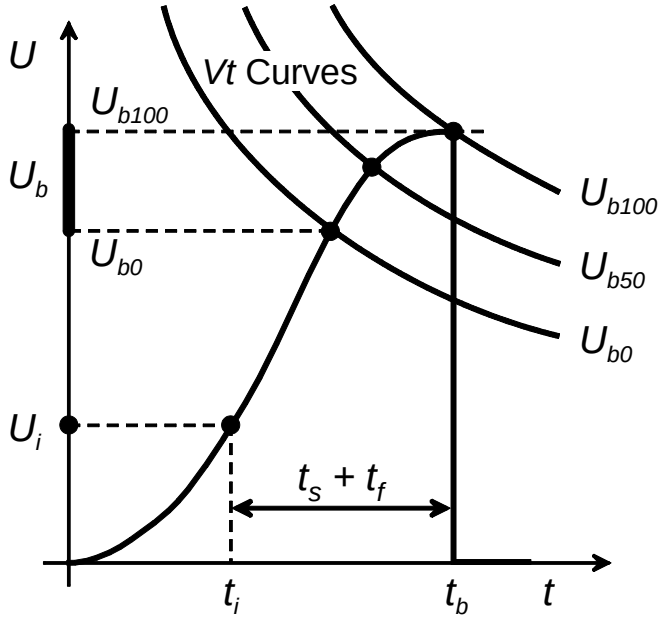

Fig. 8: *Streamer inception, breakdown voltage and the resulting V-t-curves for 0%, 50% and 100% breakdown probability in case of impulse voltages.*

The third condition for breakdown is the formation of a streamer and leader channel, which bridges the gap length between electrodes. In the case of slightly inhomogeneous fields with field enhancements in tiny regions at the surface roughness peaks usually found in high voltage equipment, the condition is met for an immediate streamer and leader formation at the streamer inception voltage U_i and the time t_i. There will be a further time lag t_f for this formation process, which causes an additional increase of the breakdown value in the case of impulse voltages. Experience has shown that for N_2/SF_6 mixtures of equal dielectric strength, the total increase of the impulse breakdown voltage is merely impulse shape dependent. Voltage-time-curves are substantially influenced by these time lags, but they are identical for such mixtures and SF_6 of equal dielectric strength, and can be applied as usual for insulation co-ordination.

5. INSULATION PROPERTIES AND DIMENSIONING OF THE INSULATION

In the case of the almost homogeneous fields due to the designed electrode curvatures, and with field enhancements caused by the usual surface roughness, the leader will be launched and breakdown may already occur at discharge inception. The corresponding minimum breakdown voltage will only depend on the critical field, and is therefore the same for N_2/SF_6 mixtures of equal intrinsic dielectric strength since the value K/k in Equ. (8) and in Fig. 2 is constant for such mixtures. There are also constant enhanced breakdown values for impulse voltages of the same shape and amplitude due to the same time lags for the breakdown channel formation. This is shown in Fig. 9 for 5 different strengths and a sphere-sphere electrode arrangement (sphere radii 125 mm, gap length 20 mm) with a maximum roughness of (8 ... 16) µm. The influence of electrode curvature (chapter 5.1) and roughness (chapter 5.2) can be estimated. In the case of strongly inhomogeneous fields at defects, leader breakdown will occur mostly beyond the discharge inception at leader inception, which depends in such mixtures on the pressure (chapter 5.3).

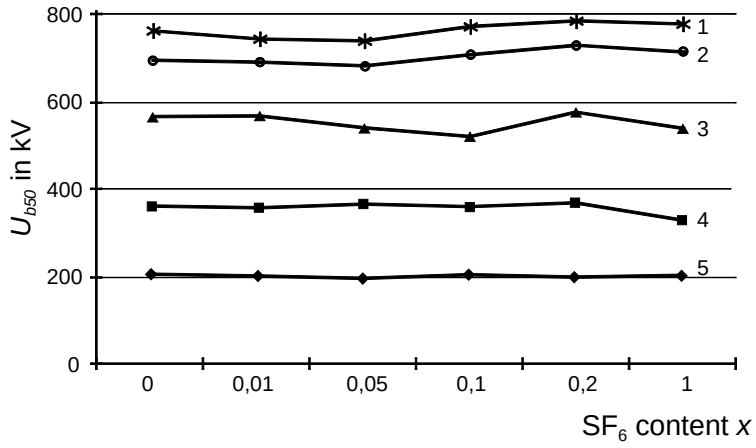

Fig. 9: *Measured 50% LI breakdown voltage for mixtures of 5 intrinsic dielectric strengths with the corresponding critical voltages U_{cr} 1: 914 kV 2: 831 kV 3: 582 kV 4: 332 kV 5: 166 kV[11].*

5.1 Influence of slight field inhomogeneities due to the design

In real equipment the field distribution is mostly slightly inhomogeneous. Therefore a simple criterion is usually applied for the calculation of the minimum breakdown voltage. It is assumed that breakdown occurs at the voltage U_{cr}, when the maximum field E_m has the value E_{cr}. Only the maximum field at the electrode surface is required for this calculation, but the real breakdown values at E_{mi} and U_i are slightly above E_{cr} and U_{cr}. More accurate results are obtained by the discharge inception criterion and simple models of the field distribution near the electrode surface. Discharge inception will occur according to Equ. (8) and (9) when the hatched voltage area in Fig. 2 has the value $K/k = 0{,}380\ kV$. The field is enhanced at electrode surfaces with convex curvature, which exist predominantly at internal live parts. Fig. 2 shows such a field ahead of a curved electrode. The electrode curvature can often be modelled by a sphere or cylinder with radius R. The corresponding non-linear field distribution can be approximated by a linear function [12]

$$E(l) = E_m(1 - 2Hl) \qquad (12a)$$

with the curvature factor

$$H = 1/2R \qquad (12b)$$

for cylindrical curvatures and

$$H = 1/R \qquad (12c)$$

for spherical curvatures. The linear approximation by Equ. (12a) is sufficiently accurate for

$$Hl \le 0{,}1 \qquad (13a)$$

Thus we get from Equ. (8) and (12a) the streamer inception criterion [7]

$$\frac{E_{cr}}{E_{mi}} + \frac{E_{mi}}{E_{cr}} = 4\frac{K}{k(E/p)_{cr}}\frac{H}{p} + 2 \qquad (14a)$$

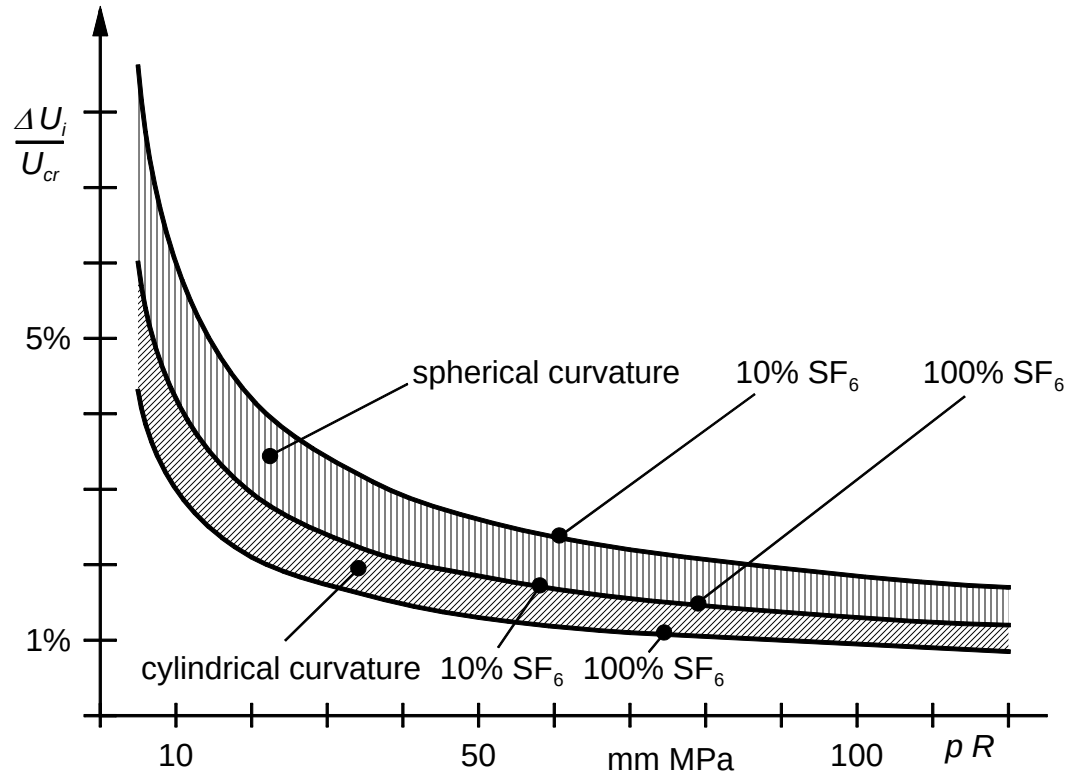

Fig. 10: *Normalized enhancement $\Delta U_i / U_{cr}$ of the discharge inception and minimum breakdown voltage at the pressure p due to electrode curvatures with radii R [7].*

Discharge inception will occur when the maximum field E_m at the electrode exceeds E_{mi}. Applying the intrinsic dielectric strength E_{cr} and the corresponding voltage U_{cr} as reference values, the relative enhancement of the discharge inception and minimum breakdown voltage $\Delta U_i / U_{cr}$ becomes

$$\frac{\Delta U_i}{U_{cr}} = \frac{E_{mi}}{E_{cr}} - 1 \qquad (14b)$$

This is presented in Fig. 10 for cylindrical and spherical curvatures. According to Equ. (13a), (14b) and (12a) the results are valid for enhancements

$$\Delta U_i / U_{cr} \le 25\% \qquad (14c)$$

At some locations especially in medium voltage equipment relatively small curvature radii and gas pressures are in use. Enhancements of some percent can be used for the design. In these cases it may be better to calculate the discharge inception and breakdown voltage by Equ. (8), where the real field distribution near the electrode has to be considered. However, for the usual curvatures and pressures of high voltage equipment the enhancement is mostly less than 2% and can be neglected, or estimated by Fig. 10 or 11. According to Equ. (14a) the so-called factor of merit

$$M = \frac{K}{k\left(E/p\right)_{cr}} \qquad (15)$$

is decisive for this phenomenon. For mixtures of high intrinsic dielectric strength the enhancement is low. It depends on *K*/*k* and for mixtures of equal dielectric strength is therefore independent of the SF_6 content and the pressure as shown in Fig 11.

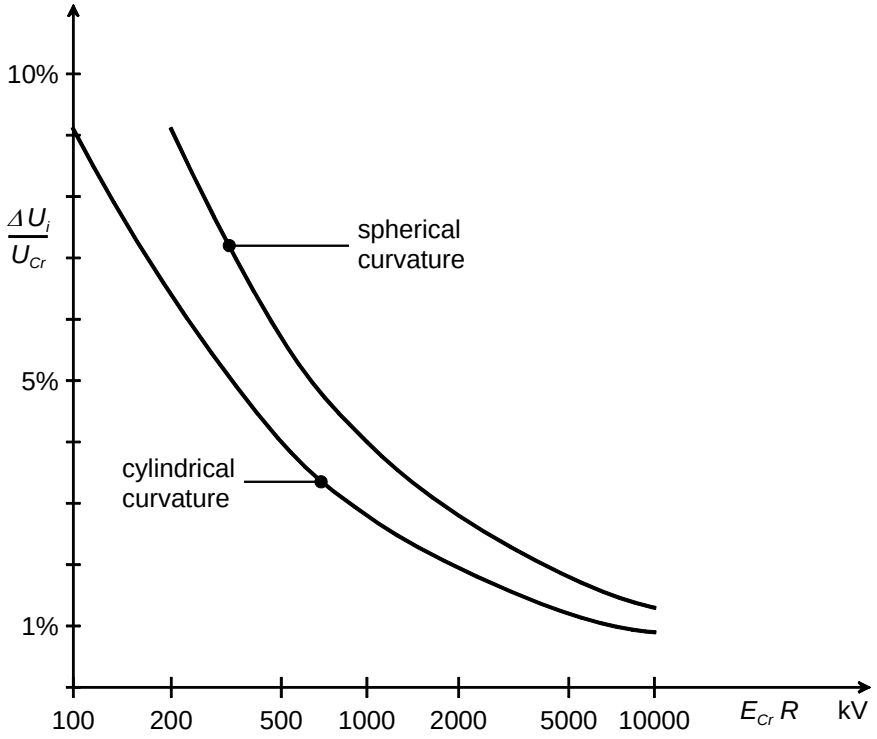

Fig. 11: *Relative enhancement of the discharge inception and minimum breakdown voltage* $\Delta U_i / U_{cr}$ *for electrode curvature radii R in* N_2/SF_6 *mixtures of known dielectric strength* E_{cr} *(independent of pressure and* SF_6 *content) [7].*

5.2 Influence of surface roughness

Field enhancement caused by surface roughness of the electrodes may cause a considerable reduction in the discharge inception and minimum breakdown voltage. These field enhancements cannot be taken into account by field calculations, but have to be estimated and considered by the chosen withstand voltage. For such estimations the surface roughness has to be modelled. By a similar calculation to that for curved electrodes, the reduction factor m of the discharge inception field or voltage

$$m = \frac{E_i / p}{(E/p)_{cr}} = \frac{U_i}{U_{cr}} \qquad (16a)$$

can be gained by

$$f(m) = \frac{M}{p} H \qquad (16b)$$

The function $f(m)$ depends by the curvature factor (Equ. (12b) and (12c)) of the shape of the assumed protrusion modelling the roughness. Mostly in use are small semi-spherical protrusions with the radius R on a plane electrode (Fig. 2) [13]. In this case $f(m)$ and H become

$$f(m) = 1 - \left(\frac{27}{4} m(1-m)^2 \right)^{\frac{1}{3}} \qquad H = 1/R \qquad (16c)$$

The reduction factor *m* is dependent only on the product *pR* and the factor of merit *M* (Fig. 12). There is no reduction at all for values of *pR* up to *M*. But for higher values considerable reductions have to be accepted which increase little with the SF_6 content. The insulation of a real N_2/SF_6 insulated component exhibits a corresponding reduction of the withstand capability (Fig. 13). The withstand capabilities are enhanced by the influence of the time lag in the case of the applied LI impulse test voltage, and therefore slightly exceed the intrinsic dielectric strength.

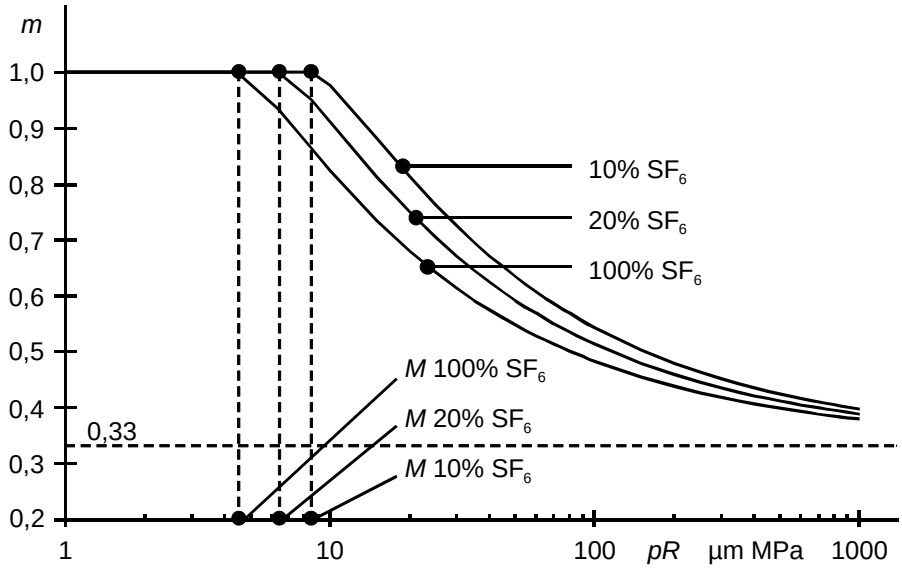

***Fig. 12**: Reduction factor m for the discharge inception and minimum breakdown voltage due to surface roughness [7].*

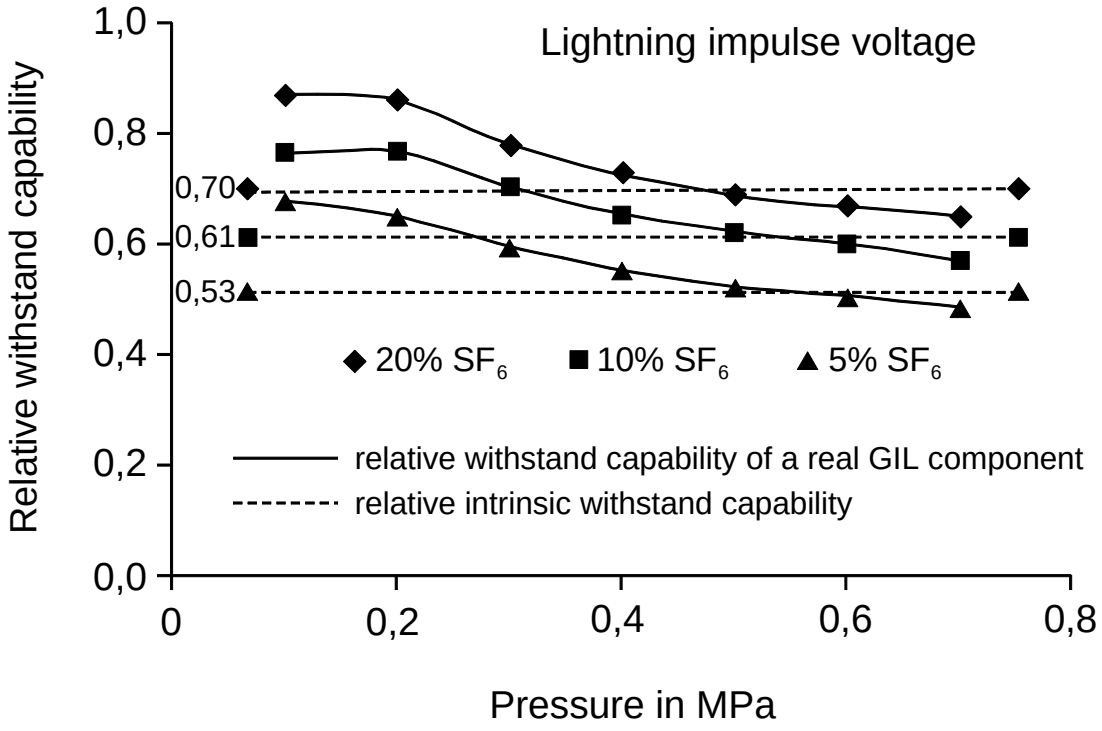

***Fig. 13:** Relative LI withstand capability of a real GIL component and the relative intrinsic withstand capability of N_2/SF_6 mixtures [14].*

For mixtures of equal intrinsic dielectric strength (E_{cr} = const) the reduction factor is constant (Fig. 14) since from Equ. (16b), (15) and (12c) the result is

$$f(m) = \frac{K}{k}\frac{1}{E_{cr} \cdot R} \qquad (16d)$$

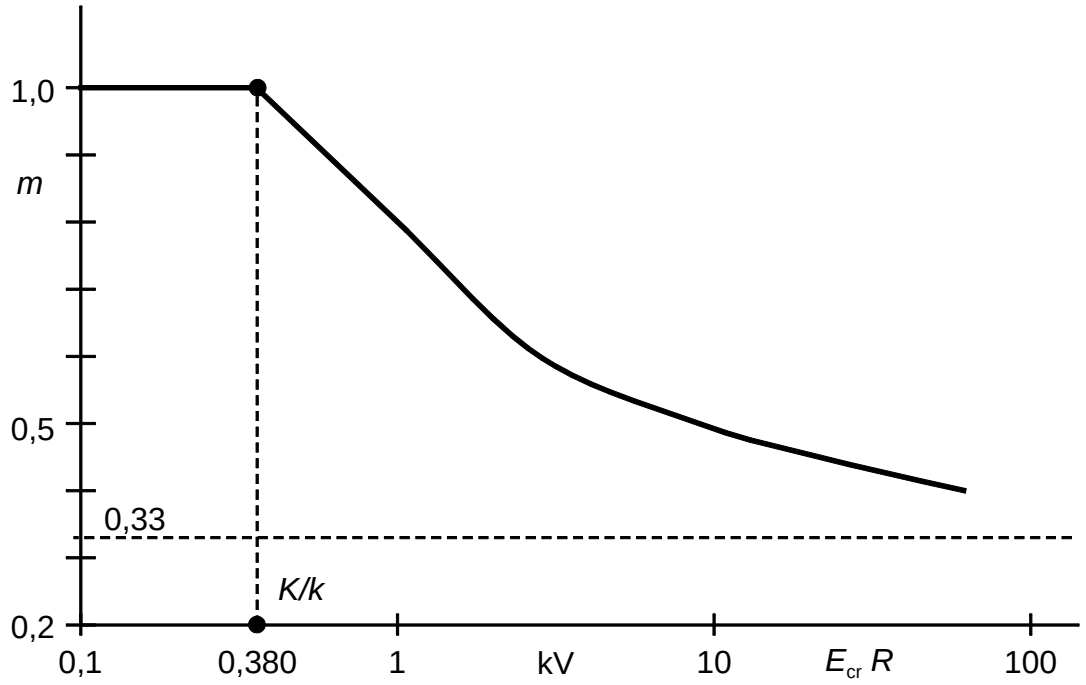

Fig. 14 : *Reduction factor m for the discharge inception and minimum breakdown voltage due to surface roughness for N_2/SF_6 mixtures of known dielectric strength (independent of pressure and SF_6 content) [7].*

5.3 Influence of severe irregularities (defects)

In the case of more severe irregularities like a needle shaped protrusion, the strongly inhomogeneous field results in a considerable reduction of the discharge inception voltage. However, breakdown may require a further increase in voltage because of the enhanced leader inception field and possible additional corona stabilization (Fig. 15).

For mixtures of equal intrinsic dielectric strength the discharge inception voltage U_i is constant provided it is not enhanced by corona stabilisation at low pressures. Below U_i there is no discharge activity at all, since discharges start at streamer inception. However breakdown can occur only when the leader inception voltage U_{iL} is also exceeded. Note that U_{iL} decreases as the pressure increases at lower levels of SF_6 content. Above the critical pressure p_{cr} there will be immediate leader inception and breakdown at streamer inception, without any discharge activity. At lower pressures (higher SF_6 content) leader inception occurs beyond streamer inception. In the case of AC stress, the discharge activity between streamer and leader inception permits PD measurements. Intensive ionisation, ion drift, charge accumulation and corona stabilization increase the breakdown voltage to U_{bC}. Therefore the breakdown level is higher in this region than under LI stress, for which corona stabilization is much smaller or may not occur at the minimum LI breakdown voltage $U_b = U_{iL}$.

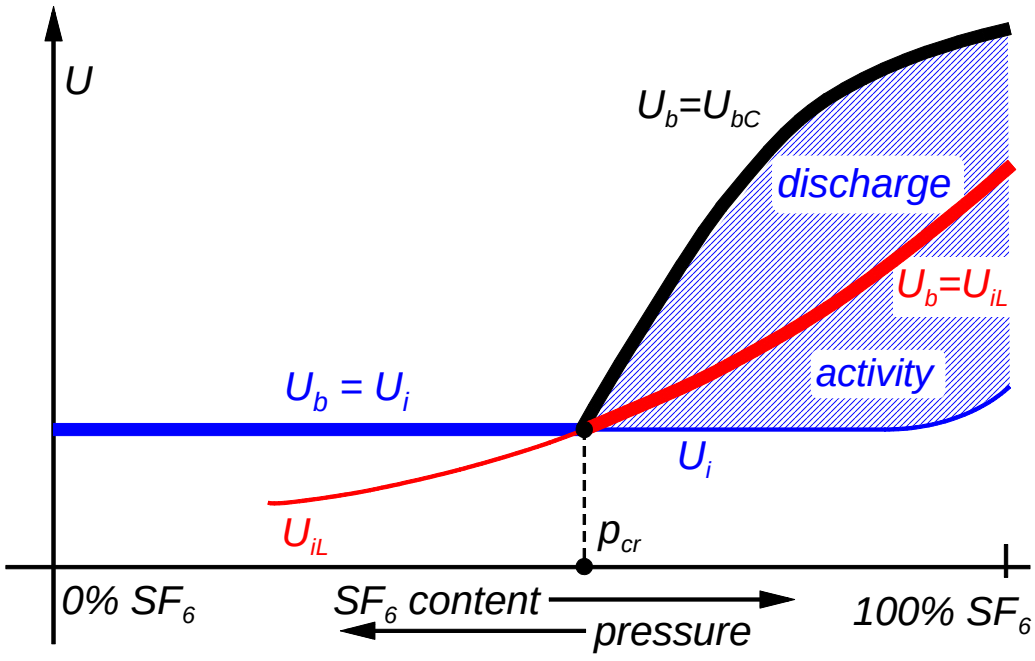

Fig. 15: *Discharge (U_i) and leader (U_{iL}) inception voltage, the corresponding minimum breakdown voltage U_b and the breakdown voltage U_{bC} in case of corona stabilization in N_2/SF_6 mixtures of constant intrinsic dielectric strength [7].*

Experimental results for mixtures of equal dielectric strength under LI stress are presented in Fig. 16 and 17, while those for AC stress are given in Fig. 18a. In Fig. 16, the critical pressure is about 0,95 MPa at an SF_6 content of 5%. Above this pressure, breakdown takes place at an almost constant value at streamer inception [11]. All breakdowns in Fig. 17 are caused at leader inception beyond streamer inception and below the critical pressure. For AC stress (Fig. 18a), the critical pressure is about 0,9 MPa at an SF_6 content of (5-10)%. The enhancement of the breakdown voltage at lower pressures is much greater than for LI stress, due to the corona stabilization effect. In this example, PD measurement would not be possible for SF_6 contents below 10%. Fig. 18b presents results for mixtures of equal pressure. In this case breakdown exceeds streamer inception in the same degree for all SF_6 contents between 10% and 100%. Below an SF_6 content of 5% the discharge process changes totally and no PD measurements can be made because streamer inception causes immediate breakdown. Due to the extremely high field inhomogeneity at such extraordinarily severe defects the calculated critical voltage U_{cr}, with a maximum field E_{cr}, is considerably below discharge inception.

As with surface roughness, the influence of defects like protrusions will affect the withstand level. However, critical protrusions at live parts rarely occur in modern GIS and are even more uncommon in the comparatively plain design of a GIL. Furthermore, only very few would not exhibit PD activity. Defects on the surfaces of insulating components affect the insulation properties of mixtures in a manner similar to SF_6 of equal intrinsic dielectric strength. Far more important are mobile particles, which may move to live parts and cause breakdown [18]. During their motion, these particles cause high PD activity by the rapid charge exchange at impacts, a process independent of the insulating medium. Therefore the PD characteristics are the same as for SF_6 insulation and all existing measures for defect diagnosis can be employed.

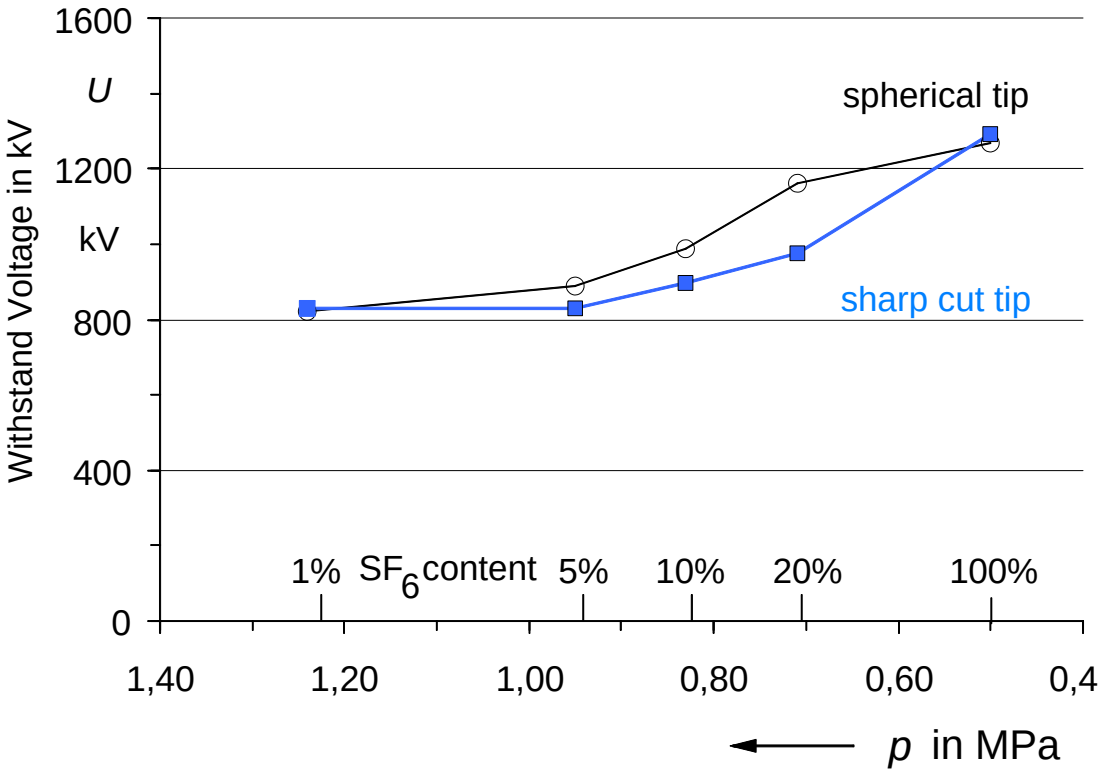

Fig.16: *Positive LI withstand voltage in case of 3 mm long protrusion for N_2/SF_6 mixtures of equal intrinsic dielectric strength and plane/plane electrodes with a gap width of 160 mm [15].*

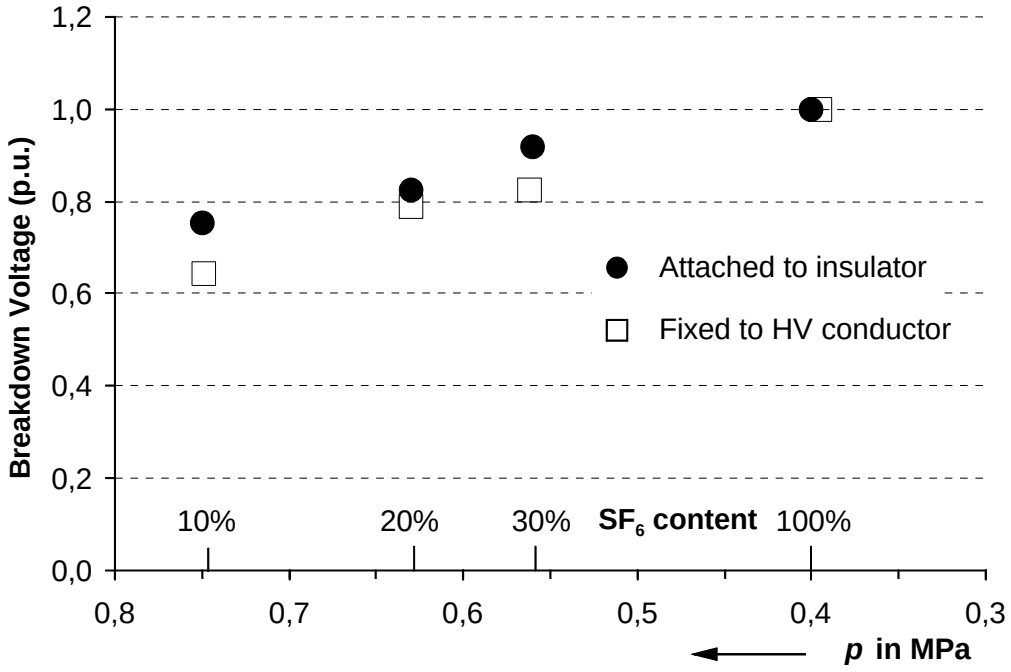

Fig. 17: *Positive 50% LI breakdown voltage in p.u. in case of 3 mm long protrusions for N2/SF6 mixtures of equal intrinsic dielectric strength [16] in a bus 340/125 mm ∅.*

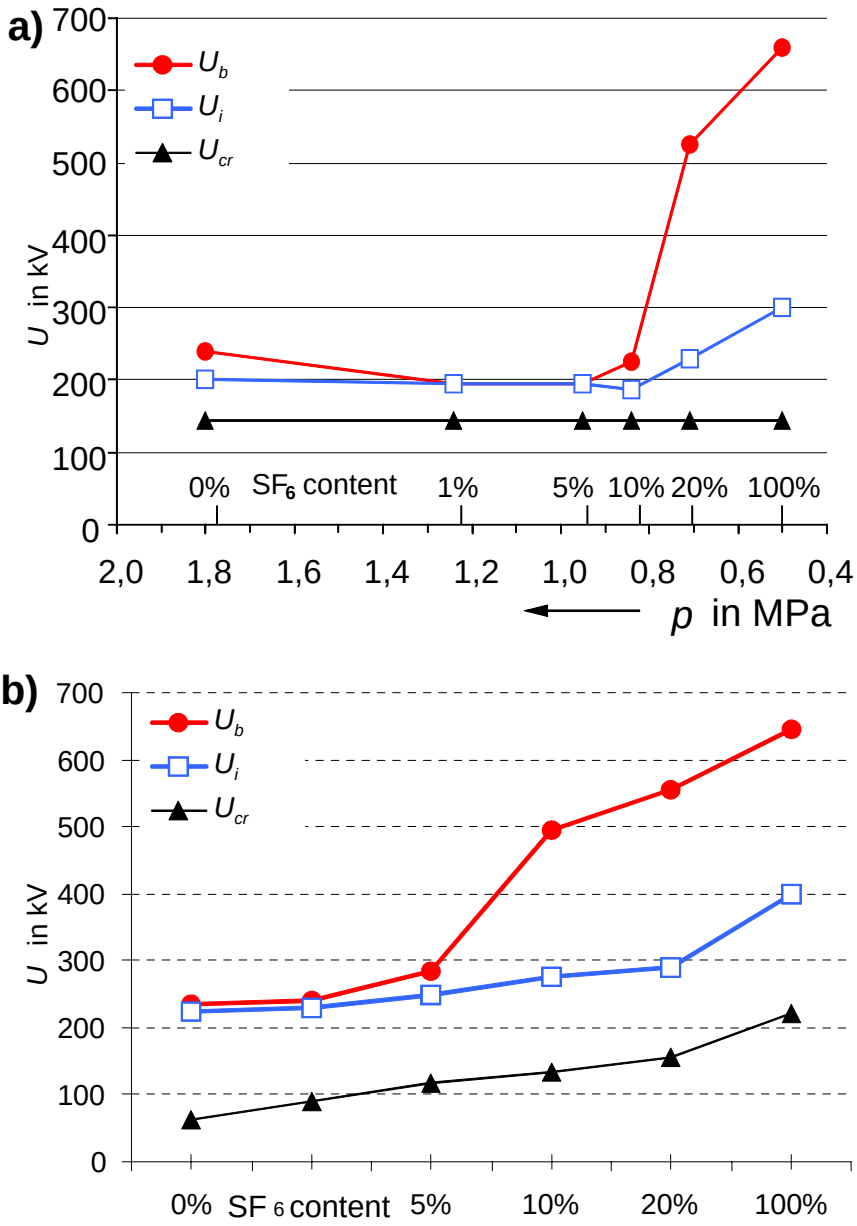

Fig. 18: *AC breakdown voltage U_b measured (Photomultiplier) discharge inception U_i and calculated critical voltage U_{cr} for N_2/SF_6 mixtures of equal dielectric strength. Setup as for Fig. 16 but using a sharp cut protrusion 10 mm long [17].*

a) N_2/SF_6 mixture of equal dielectric strength

b) N_2/SF_6 mixture of equal pressure p=0,5 MPa

6. DIAGNOSTICS

PD diagnostic systems developed for equipment filled with pure SF_6 can be applied in the same way for equipment containing N_2/SF_6 mixtures. In the following discussion, the application of these methods is dealt with for the two most important defect types, fixed protrusions and moving particles. Identification and localization of discharging defects in SF_6 and N_2/SF_6 gas mixtures are similar in principle, and are not discussed here. More details can be found in [19,20].

6.1 Detection methods

To detect PD in GIS using pure SF_6 the following PD measurement methods are used [19]:
- conventional measuring systems based on the IEC 60270 recommendations;
- acoustic measurements using externally mounted acoustic sensors which detect the acoustic signals emitted by a PD source [21];
- UHF measuring systems using narrowband or wideband filters, with detection in a frequency range up to several GHz. Systems have been introduced over the last decades during on-site tests [22-25];
- methods based on chemical effects of PD processes [26], however these are not sensitive enough due to the large amount of gas;
- methods based on the optical properties of discharges [26] which are mainly used for identification of internal arcs, and only in the academic world for PD detection.

In case of gas-mixtures the same detection methods can be applied.

The conventional method can be applied as long as the equipment can be considered as a lumped capacitance. Depending on the frequency bandwidth, the method is applicable for (shipping) units of several tens of meters. It is independent of the gas used for insulation, and is valid for all types of defects. With this method the apparent charge is measured. The acoustic method [27] can be applied for PD measurements in gas mixtures. Discharges generate acoustic signals similar to those in pure SF_6. Although the mixtures have different acoustic transfer properties (i.e. the acoustic impedance), they do not affect the signals markedly. The UHF method [23] can successfully be applied for PD measurements in gas mixtures [28].

In N_2/SF_6 gas mixtures with a minimum SF_6 content of 5% (in practice 10-20% SF_6 content is used) the discharge currents of fixed protrusions are quite similar to those of pure SF_6. Discharges of electrodes with floating potential are usually very severe, and can easily be detected by all methods independent of the gas mixture. In the case of free particles, the dominant process is charge exchange during the mechanical impact with the enclosure. Voids in solid materials (e.g., epoxy resin spacers) often contain a gas that originates from the casting process and is independent of the insulation gas. Consequently, the nature of the PD signals is not affected. Therefore the use of a gas mixture has little influence on the potential for PD detection.

6.2 Comparison of sensitive detection in pure SF_6 and mixtures

With the UHF PD measuring method, a frequency spectrum is measured at one of the couplers inside the GIS. The shape of this frequency spectrum, as obtained with a spectrum analyser, looks rather arbitrary and depends on the structure of the GIS, location of the defect and type of coupler. Fig. 19 shows examples of spectra measured at 20% or 75% above the discharge inception voltage U_i for different defects in N_2/SF_6 gas mixtures and pure SF_6 of equal dielectric strengths (pure SF_6 at 0,45 MPa; 10% SF_6 – 90% N_2 gas mixture at 0,75 MPa; and 5% SF_6 – 95% N_2 gas mixture at 0,95 Mpa). For further analysis of frequency spectra, statistical methods can be applied [20].

Fig. 19 shows the sensitivity of the UHF measuring technique to defects in pure SF_6 and N_2/SF_6 gas mixtures, in which the UHF signal spectrum has been measured at a coupler inside the GIS. It can be concluded that there is no difference for free moving particles. The frequencies present in the spectra are quite similar for fixed protrusions in gas mixtures and in pure SF_6, but their amplitudes differ considerably. Higher signals have been recorded in mixtures. However, the data in Fig. 18 show that for SF_6 content below 10% in the gas mixture, the difference between the PD inception voltage and breakdown may be very small. Although a higher sensitivity in mixtures can be observed, the reduced margin to breakdown has to be recognized.

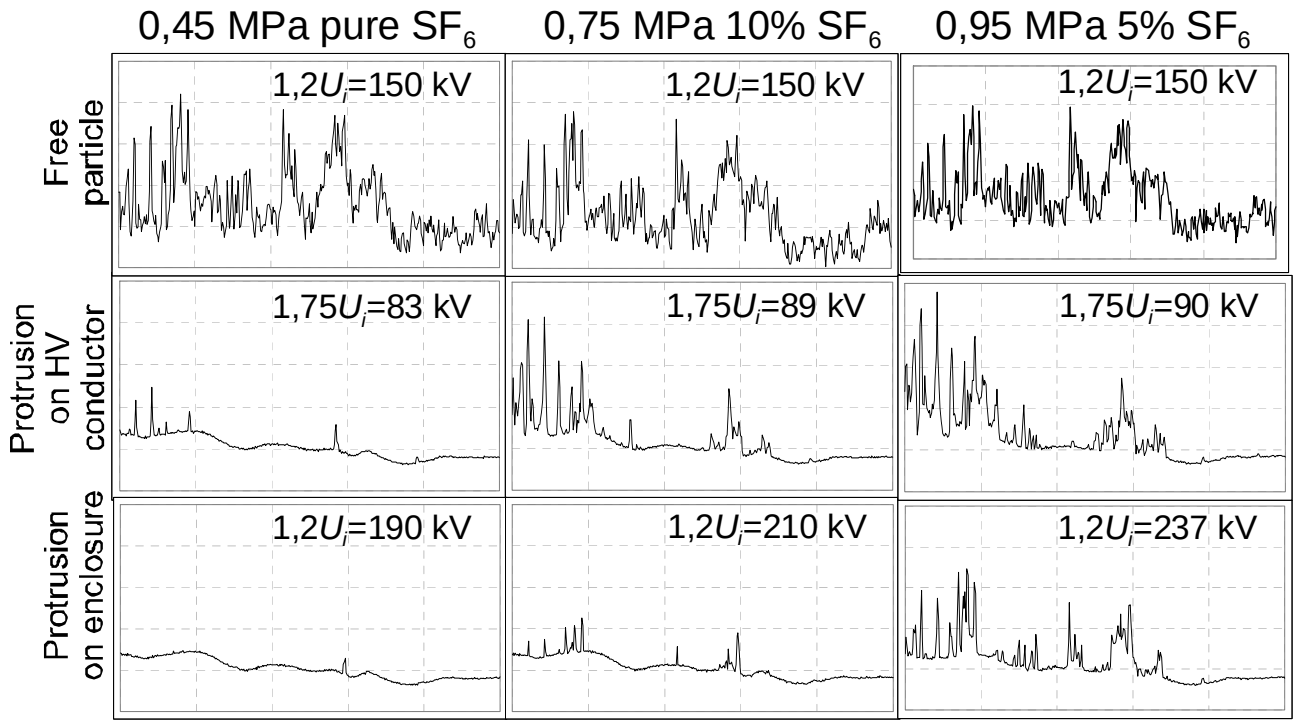

Fig. 19: *Examples of UHF spectra in the frequency range of 0,1–1,6 GHz for different defects in pure SF_6 and N_2/SF_6 mixtures of equal intrinsic dielectric strength. Defect types: 10 mm free particle (vertical scale –50 to –100 dBm), 15 mm protrusion on conductor (vertical scale –60 to –110 dBm), 30 mm protrusion on enclosure (vertical scale –60 to –110 dBm).*

6.3 Examples of different types of PD patterns

6.3.1 Phase resolved PD patterns

Correlating the PD signals to the 50/60 Hz waveform of the applied voltage results in one form of phase-resolved PD patterns (PRPD patterns, Fig. 20). There exists a relationship between the shape of the PRPD patterns and the discharge source (type of defect) [29]. Each discharging defect with its geometry, location in insulation, dielectric properties and local field is characterised by a specific PD sequence. Analysis of these patterns is a good method for distinguishing different types of defect [29].

PRPD patterns can be obtained using the UHF method, the acoustic method or the conventional method. Fig. 20 shows examples of PRPD patterns for different defects recorded at 20% or 75% above the discharge inception voltage U_i with the narrow band UHF method, in different gases at equal dielectric strengths. In each case the spectrum analyser for the narrow band UHF method was tuned to the centre frequency shown, and a resolution bandwidth of 3 MHz was used. The protrusions investigated had a tip-radius of about 100 µm. The protrusion fixed to the high-voltage conductor (HV-protrusion) was 15 mm long; the protrusion fixed to the enclosure (LV-protrusion) 30 mm. The mobile particle used was 10 mm long.

It can be concluded that the type of gas and its pressure has no influence on the PD magnitude (pC) obtained using free particles. In the case of fixed protrusions, differences can be observed. Moreover, similar shapes of the PRPD patterns have been observed using an IEC 60270 measuring circuit and the narrow band UHF method [30].

It is not possible to correlate the measured narrow band UHF signal to the actual size of the defect, or the apparent charge according to the IEC 60270. The measured magnitude of the UHF discharge pulses strongly depends on the measuring configuration, type of defect and resonances inside the GIS. However, disregarding the recorded magnitude (µV), the shapes of the patterns obtained with a free particle are very similar. This is of importance for PD defect recognition methods. In contrast, the PD magnitude recorded with a measuring circuit according to the IEC 60270 recommendations can be calibrated, and the PD magnitudes (pC) are given in Fig. 20.

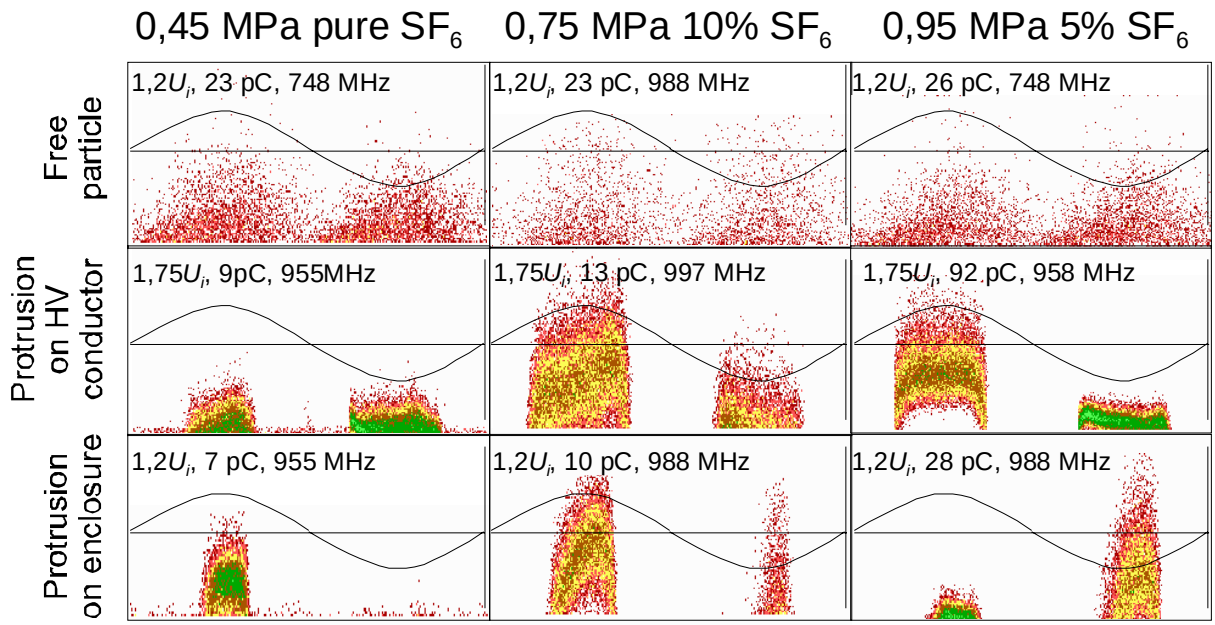

Fig. 20: *Examples of phase-resolved PD patterns using the narrow band UHF method for different defects in pure SF_6 and N_2/SF_6 mixtures of equal intrinsic dielectric strength. Defect types: 10 mm free particle, 15 mm protrusion on conductor, 30 mm protrusion on enclosure. The PD pulse density is indicated by the colour.*

6.3.2 $\Delta u/\Delta\varphi$ and Δu PD patterns

Besides the most commonly used PRPD diagnosis tool for defect identification, other tools like the voltage difference Δu and voltage gradient $\Delta u/\Delta\varphi$ diagnostic procedures are increasingly offered. However the corresponding patterns are similar in N_2/SF_6 mixtures and pure SF_6, for the same defect type, as shown in Fig. 21 for mobile particles and protrusions at the HV conductor or on the surface of insulators [31]. Therefore the common diagnostic systems for defect identification can be applied for N_2/SF_6 mixtures in the same manner as for pure SF_6. The major advantage is that normally only one reference data base for computer aided defect identification is necessary.

In the $\Delta u/\Delta\varphi$-pattern (Fig. 22) the slope $m_i=[u(\varphi_i)-u(\varphi_{i-1})]/[\varphi_i-\varphi_{i-1}]$ approximates the voltage gradient which is necessary to excite a consecutive PD pulse. When the frequency of the slopes of consecutive PD pulses m_i and m_{i+1} are put into a co-occurrence matrix where m_i is on the x-axis, m_{i+1} on the y-axis and the frequency of a (m_i, m_{i+1}) relation is on the z-axis (indicated by spectral colour), a pattern is created. This represents - as well as the Δu-pattern - a histogram of the PD activities within the discharging area with the dominating real quantities, phase position and voltage of occurrence. The Δu-pattern [32] evaluates the frequency of the voltage differences of a sequence of PD pulses, showing the voltage range necessary to evoke consecutive PD pulses. The graph is also visualised by a co-occurrence matrix. For both types of patterns the Δu and $\Delta\varphi$ parameters in use can be measured as real quantities. For the detected PD pulses no measurement of the PD charge or of any other PD parameter is necessary because they are of no influence on the pattern.

a) ***Δu/Δφ patterns***

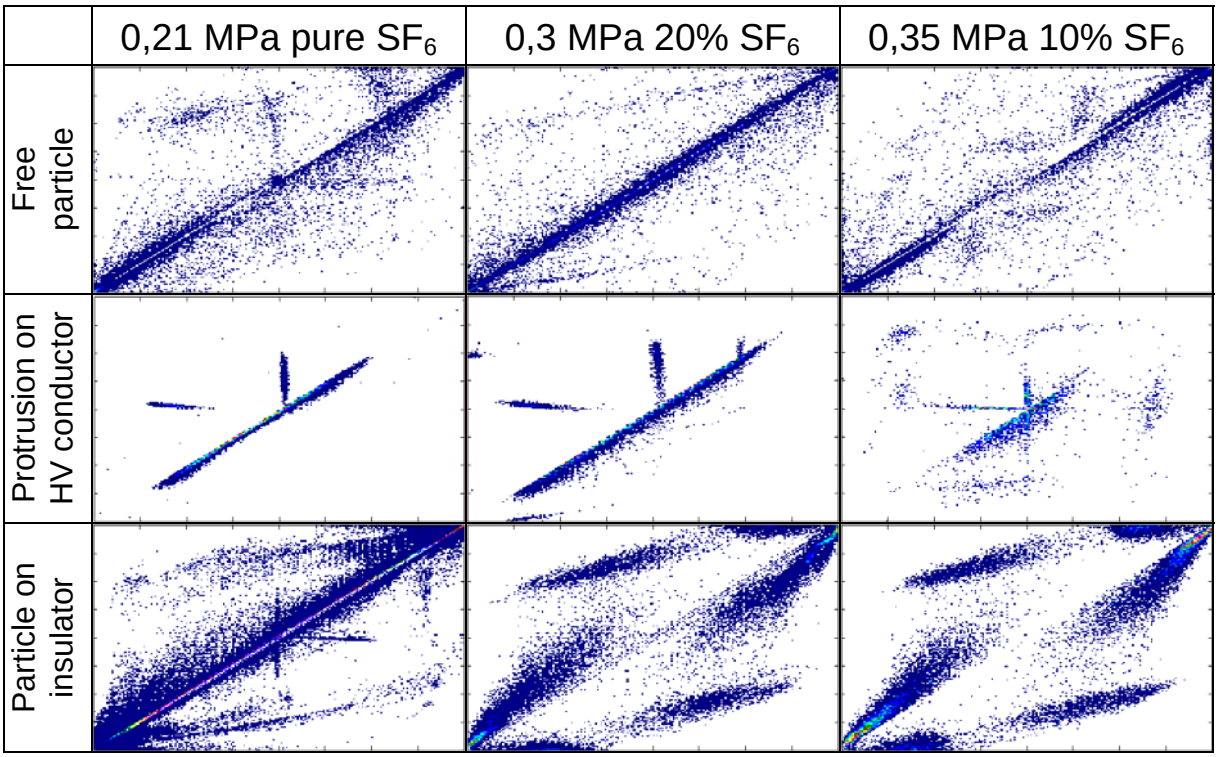

b) ***Δu patterns***

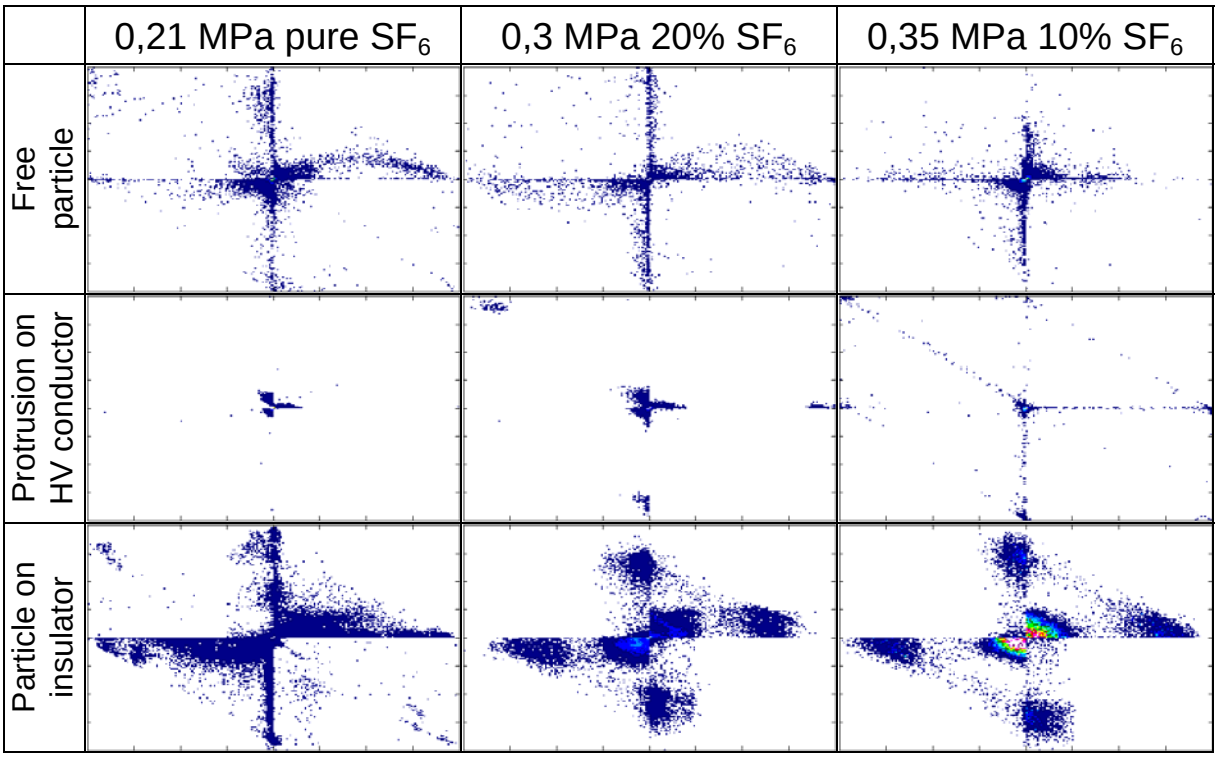

Fig. 21: *Examples of Δu/Δφ* ***(a)*** *and Δu* ***(b)*** *patterns of an approximately 3 mm long free particle, a 8 mm protrusion fixed to the conductor and a 3 mm particle fixed on an insulator in 0.21 MPa pure SF_6 and N_2/SF_6 mixtures of equal intrinsic dielectric strength.*

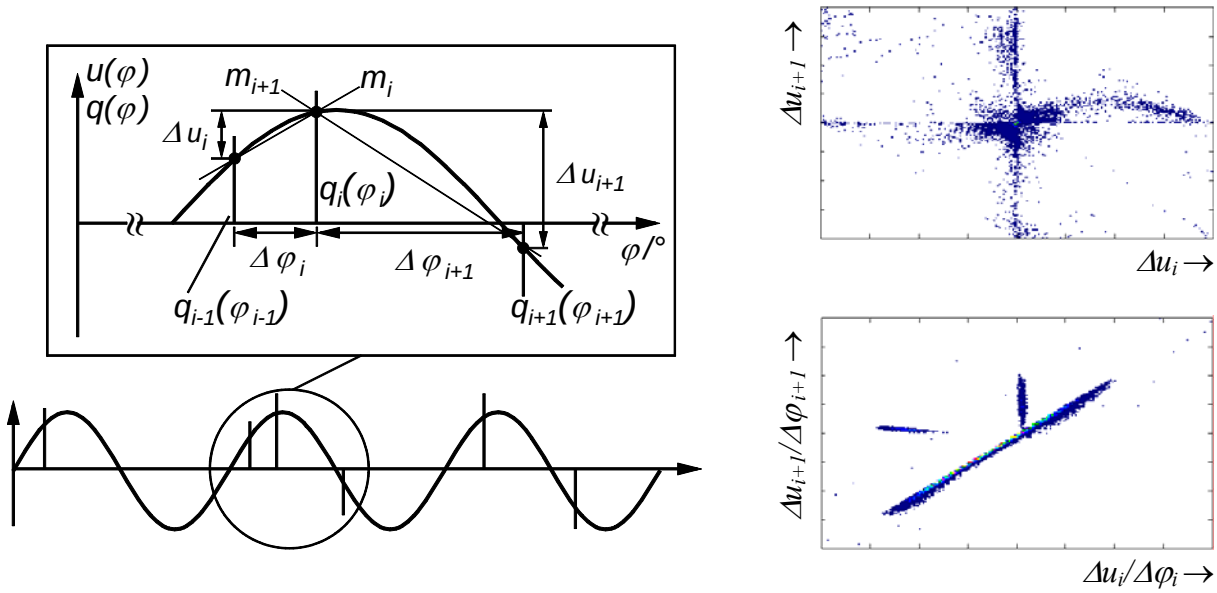

Fig. 22: *Determination of Δu- and Δu/Δφ-values to create Δu-patterns (top right) or Δu/Δφ-patterns (bottom right).*

7 DISCONNECTOR SWITCHING OF BUS-CHARGING CURRENTS

7.1 Failure mechanism

Disconnectors in GIS, as defined by IEC, have as their main operational function to isolate the circuit in the open position. They are operated under no load, but they have to interrupt at high voltages small capacitive bus-charging currents (max 500 mA), or larger induced currents with negligible voltage during bus transfer switching. In both cases no special arc extinction system is required due to the low current or voltage during the switching operation. However in the case of bus-charging currents the disconnector switching performance requires adequate properties of the insulation system, achieved by the combination of the design and the gas mixture used. Flashover to ground from the arc between contacts during the switching of bus-charging currents has to be avoided by appropriate measures, especially at higher voltage ranges (420 kV and 550 kV).

Since the disconnector is an off-load switching device, the speed of the operating mechanism is usually very slow by circuit breaker standards. Therefore there are many pre-strikes or re-strikes respectively during the closing or opening operations, especially for longer gap lengths between contacts at the higher voltage ranges. Flashover to ground was initially assumed by its appearance to be a breakdown from the completed arc between contacts. It is however caused by leader branching (Fig. 23b) during the stepwise leader propagation (chapter 4). Such branching is more probable for long leader channels with many leader steps, as found in disconnectors for high voltage operation. A sideways directed branch may be diverted radially when the main branch arrives at the opposite contact. That entails a sudden change in direction of the hitherto axial field between the contacts (Fig. 23a,b), into a radial field directed towards ground (Fig. 23c). There is also a development of very fast transient (VFT) overvoltages caused by the rapid collapse of the voltage between the contacts. Both phenomena promote leader development towards ground in the side branch (Fig. 23c,d) until flashover occurs. The collapse of the voltage and the VFT amplitude increase proportionally to the operating voltage, which additionally makes such flashover more probable at high voltages.

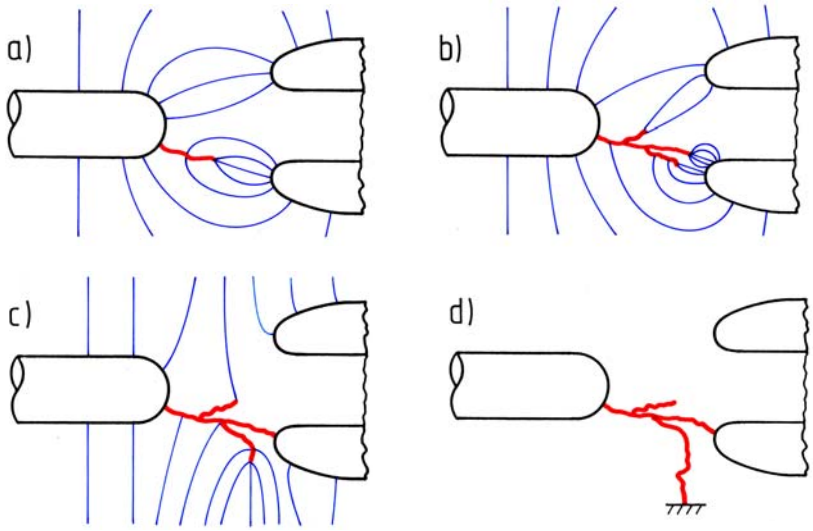

Fig. 23: *Development of the flashover to ground during a disconnector operation.*
red: paths of leader propagation
blue: electric field lines

7.2 Leader branching and failure in mixtures

The leader development depends on the pressure, and is therefore not the same in N_2/SF_6 mixtures of different SF_6 content and pressure, but of equal intrinsic dielectric strength.

A 245 kV GIS disconnector has been tested with AC voltage in a fixed open position with a gap length between contacts of 41 mm [33]. One contact was grounded while the potential of the other was raised until breakdown. Fig. 24 shows the resulting arc channels in pure SF_6 at 0,6 MPa (Fig. 24c), and in N_2/SF_6 mixtures of approximately equal intrinsic dielectric strength given by an SF_6 content of 20% at 0,9 MPa (Fig 24b), and of 10% at 1,05 MPa (Fig. 24a). Breakdown occurs within the range of 451 kV ± 5%.

Due to the moderate field inhomogeneity at the contact surfaces, leader inception and breakdown is caused at discharge inception and is almost equal for these mixtures. The small scatter is caused by the varying roughness. However the arc channels in the mixtures differ from those in pure SF_6. In SF_6 there are only a few comparatively thick, straight channels with almost no branching. In the gas mixtures there are multiple channels, which frequently depart from the shortest route by many changes in direction and branching. They are much thinner than those in pure SF_6, since the current is shared between many parallel arcs and correspondingly reduced in each channel.

The more frequent change of direction and branching of the leader in N_2/SF_6 mixtures compared with pure SF_6 of equal intrinsic dielectric strength is caused by the pressure dependence of the leader inception and stepwise leader propagation. Each new leader step is preceded by a streamer corona of the same extension (Fig. 6). It is initiated at the tip in one of the various differently directed filamentous streamers of the streamer corona, from which it takes its direction. Sometimes that happens simultaneously in two filamentous streamers. and results in leader branching. The probability P of a new leader step in the direction of the field component E at the tip of a streamer filament [34] is:

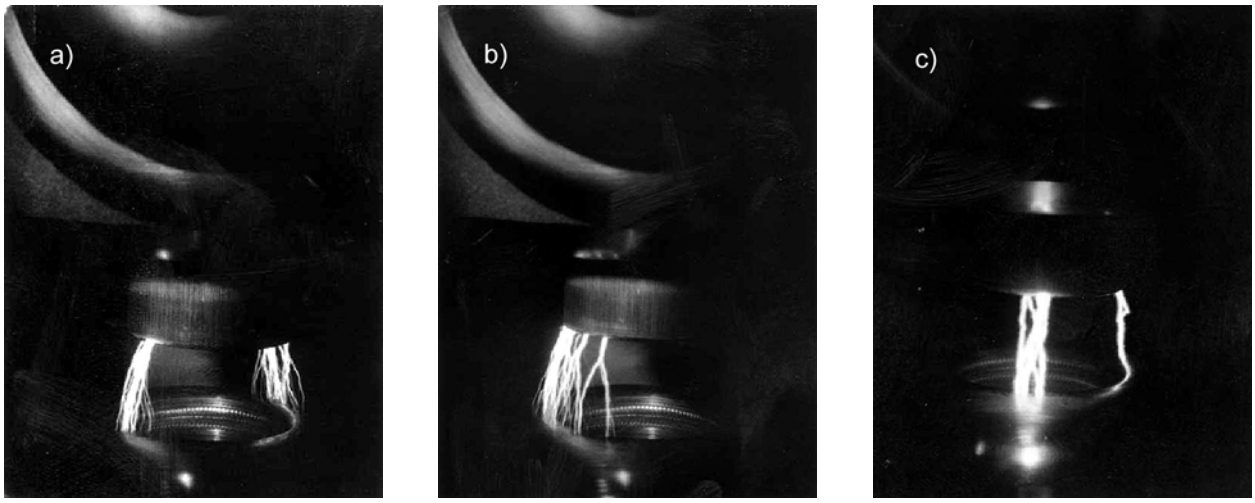

Fig. 24: *Arc channels between disconnector contacts with a gap length of 41 mm and insulation media of approximately equal intrinsic dielectric strength.*
a) *N_2/SF_6 mixture with 10% SF_6 and 1,05 MPa.*
b) *N_2/SF_6 mixture with 20% SF_6 and 0,90 MPa.*
c) *Pure SF_6 with 0,60 MPa.*

$$\begin{aligned} P &= \text{const}\left(E - E_L\right) \quad \text{for} \quad E \geq E_L \\ P &= 0 \qquad\qquad\quad \text{for} \quad E \leq E_L \end{aligned} \tag{17}$$

E_L is the threshold field for leader propagation by a new leader step. It decreases with the pressure of the gas mixture and is therefore greater in pure SF_6 than in N_2/SF_6 mixtures with equal intrinsic dielectric strength.

The ratio P_S/P_0 of the probability P_S for a sideways direction with the field component $E_S < E_0$, and of the probability P_0 for the straight direction of the maximum field E_0 comes from Equ. (17)

$$\frac{P_S}{P_0} = \frac{\frac{E_S}{E_0} - \frac{E_L}{E_0}}{1 - \frac{E_L}{E_0}} \text{ for } E_S \geq E_L \qquad\qquad \frac{P_S}{P_0} = 0 \text{ for } E_S \leq E_L \leq E_0 \tag{18}$$

and is shown in Fig. 25. The greater threshold value E_L in pure SF_6 in any case gives a higher normalized probability P_S/P_0 for a sideways directed new leader step in mixtures, than in pure SF_6 of equal dielectric strength. In the example of Fig. 25 P_S/P_0 is zero for pure SF_6.

In addition to this enhanced probability for changes in direction of leader steps in N_2/SF_6 mixtures, there are also more individual leader steps than in pure SF_6 of equal intrinsic dielectric strength. That is caused by the reduced step length in mixtures due to the higher pressure, which reduces the critical streamer extension and the leader steps. Changes in direction are therefore much more frequent, and result in more divergent paths for the re- and pre-strike arcs. Since any leader branching provides an opportunity for the directional change of at least one of the new leader steps, the probability of the leader branching will be higher in gas mixtures. That increases the probability of flashover to ground, which is also enhanced by the divergent leaders, since they are less centred on the disconnector axis where the radial field to ground is lowest.

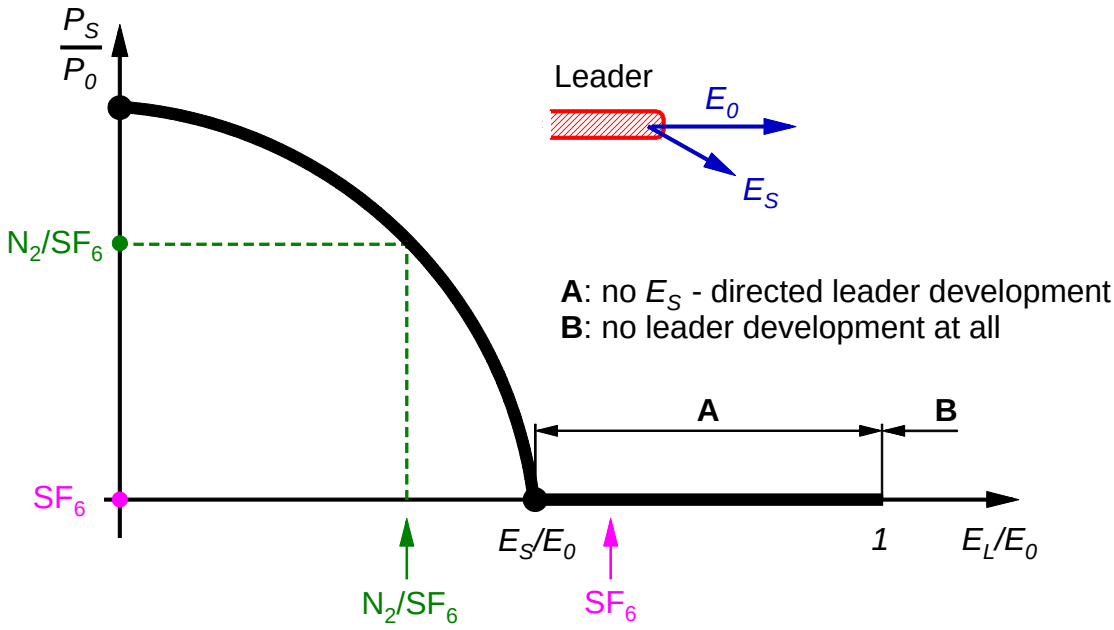

Fig. 25: *Normalized probability P_S/P_0 for a change of the next leader step into direction of E_S in SF_6 and N_2/SF_6 of equal intrinsic dielectric strength with examples in green (SF_6) and pink (N_2/SF_6) colour.*

Furthermore, the worse behaviour is caused by the low leader breakdown voltage due to the high pressure in these mixtures. After the collapse of the voltage between the contacts, the radially diverted branch of the leader is stressed by the field to ground due to the high VFT overvoltages. The field distribution at the tip of the side branch is strongly inhomogeneous, like that of a needle shaped protrusion where the leader inception criterion is decisive for leader propagation and breakdown. Therefore the breakdown voltage to ground decreases with the pressure in such mixtures, and is lower in N_2/SF_6 mixtures than in SF_6 of equal intrinsic dielectric strength.

7.3 Disconnector performance in gas mixtures

The probability of such flashovers has been tested in the same test 245 kV GIS disconnector set-up. In this case, the fixed contact was not grounded but left floating [33]. Fig. 26 compares the arc channels for two gas mixtures, and pure SF_6 at pressures giving approximately equal intrinsic dielectric strength. Flashovers occurred in the mixture with 10% SF_6 (Fig. 26a) at 343 kV and 21mm gap length, and in the mixture with 20% SF_6 (Fig. 26b) at 375 kV and 31 mm gap length. In pure SF_6 (Fig. 26c) no flashover to ground occurred, even during many more tests at a gap length of 41 mm and 420 kV.

The VFT overvoltage which promotes the leader development to ground is proportional to the collapse of voltage between contacts, and caused by the resulting superimposed surges at the disconnector due to multiple reflections within the GIS. It therefore depends on the GIS design and layout, and the residual voltage of the floating contact due to the trapped charge caused by preceding switching operations.

The standard IEC 61259 defines a procedure for testing the disconnector switching performance for bus-charging currents in a GIS under worst case conditions [35]. An SF_6 insulated disconnector passed the test for both 550 kV and 420 kV levels [36]. When the 420 kV test was repeated with a N_2/SF_6 mixture (20% SF_6) of approximately equal intrinsic dielectric strength, there were two flashovers to ground during just 17 closing operations. In contrast, with pure SF_6 the required 50

switching operations were performed successfully at 420 kV. The switching performance in a real GIS containing a N_2/SF_6 mixture is therefore much worse than in an SF_6 insulated GIS.

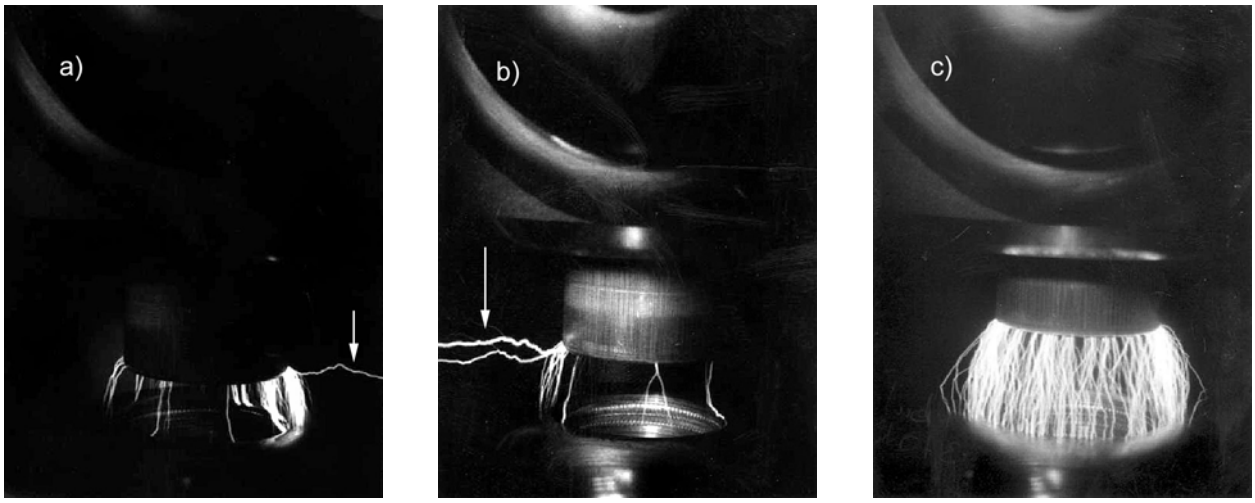

Fig. 26: *Arcs in a disconnector with insulation media of approximately equal intrinsic dielectric strength (flashover to ground indicated by arrows).*

a) N_2/SF_6 mixture with 10% SF_6 and 0,85 MPa
342 kV breakdown voltage between contacts with 21 mm gap length.

b) N_2/SF_6 mixture with 20% SF_6 and 0,70 MPa
375 kV breakdown voltage between contacts with 31 mm gap length.

c) Pure SF_6 with 0.40 MPa
420 kV breakdown voltage between contacts with 41 mm gap length.

8 FURTHER ESSENTIAL PROPERTIES

8.1 Decomposition products

As insulating gases, both N_2 and SF_6 are chemically inert. Mixtures of the two are chemically stable under normal conditions. Nevertheless, when subjected to electrical discharges (corona, spark, arc) and in the presence of impurities (such as oxygen or water vapour) and solid materials, N_2 and SF_6 can form various dissociation products. These products, as well as their detection and handling procedures, have been extensively studied and reported on for the two separate gases over many decades. Practical implications for SF_6 insulated equipment are given by IEC 61634, IEC 60480 (presently under revision) and CIGRE [37, 38], while N_2/SF_6-mixtures are surveyed in [2].
Several investigations with discharges in N_2/SF_6-mixtures have confirmed effects that are known in relation to the individual gases. In addition, some special effects due to the mixture of N_2 and SF_6 have been observed. As an example, many parameters influence the amount of dissociation products such as SOF_4 and HF, and the tendency is for them to become more dominant in the mixture than would be expected from the SF_6 amount alone [39,40]. Furthermore, additional gaseous decomposition products not to be found in SF_6 insulated equipment have been identified; NF_3 [4, 39, 41], N_2F_2 [4], N_2O [41]. Therefore, the existing quantitative data of decomposition products in SF_6 insulated equipment should not be assumed to apply to decomposition products in gas mixtures. However, for practical purposes, the existing precautions for handling SF_6 decomposition products and the actions applicable to the equipment (IEC 61634, IEC 60480 (presently under revision)) and CIGRE [2, 37, 38]) cover all decomposition products including the additional ones mentioned.

8.2 Effects due to internal arcs

A fault leading to arcing within GIL or GIS has a low order of probability due to the precautions taken according to IEC 61640 and IEC 62271. Nevertheless, for a thorough evaluation, internal overpressure and arc roots are considered for mixture-insulated equipment and compared with SF_6 -insulated equipment.

An internal arc is normally the severest fault condition, caused by a short-circuit between the live parts of the equipment and the grounded enclosure. The fault current i can reach several tens of kA and last for a time T of several hundreds of ms. The internal arc causes a pressure increase Δp that is usually higher in mixture-insulated equipment than in SF_6-insulated equipment. The arc energy $\int ui\,dt$ does not change very much between mixtures and SF_6, since for both the arc voltage u has been found empirically to be in the range between 0,8 and 1,4 kV [2]. The higher pressure increase in mixtures is due mainly to the higher adiabatic exponent γ of the gas mixture [2], found by interpolating approximately linearly between the values of 1,4 for N_2 and 1,07 for SF_6.. If the gas volume V is large enough – as can be expected for GIL in most cases – the overpressure is not sufficient to activate the rupture diaphragms [42]. It can be roughly calculated [2] by

$$\Delta p = \frac{(\gamma - 1)}{V} \cdot \int_T ui\,dt \qquad (19)$$

In reality the pressure rise has been measured to be lower than the one predicted by Equ. (19) [2]. The main reasons are that part of the energy is taken up by the enclosure, and that the specific heat of the SF_6 starts changing at temperatures above 1600 K [43].
When an internal arc occurs, the resulting arc roots on bare electrode surfaces of N_2/SF_6-insulated equipment (about 80% N_2 content) have been found to be much smoother compared to affected surfaces with SF_6 insulation [42]. This can be explained by the fact that the effective arc diameter is much larger in the mixture. The resultant small erosions of the enclosure usually allow auto-reclosure of a complete transmission system, including a GIL, because there is no increased danger of a burnthrough by a second power arc at the fault position [42]. However, in any case the GIL will need repair after an internal arc. The necessary precautions (mentioned in [37]) for compartments that have been subjected to an arc in SF_6 include all necessary actions to deal with the effects of possible additional decomposition products caused by the presence of high proportions of N_2 in the mixtures.

8.3 Heat transfer

Current flowing through gas-insulated equipment generates heat. According to IEC 61640 and IEC 62271 particular attention must be paid to the maximum temperature of contacts to avoid ageing phenomena. If SF_6 is to be replaced by a N_2/SF_6 gas mixture of equivalent dielectric strength, it is necessary to establish the thermal properties of the mixture relative to those of pure SF_6. Calculations may be based on the analytical approach developed for GIL by CIGRE [3,44]. The heat components generated in the main conductor and in the enclosure are considered, as well as the thermal resistances of the components of the GIL. The characteristics of the gas have to be taken into account for the thermal resistance between the main conductor and the enclosure, whereas the temperature rise of the enclosure depends mainly on the thermal resistance of the ambient medium. The size and emission factor of the surface of the enclosure are the main parameters for the temperature of the enclosure surface.

Heat transfer in gas insulated equipment occurs predominantly by radiation and convection [45,46]. Radiated heat loss is independent of the properties of the gas. The ratios of heat transfers by convection ($W_{\text{conv mix}}$ for the mixture and $W_{\text{conv SF6}}$ for pure SF_6) can be approximated by the following expression, allowing for different total pressures (p_{mix} and p_{SF6}):

$$\frac{W_{conv\,mix}}{W_{conv\,SF6}} = \frac{x+1,57}{2,57} \cdot \left(\frac{p_{mix}}{p_{SF6}} \right)^{0,6} \tag{20}$$

where x is the proportion of SF_6 content. The equation shows that heat transfer by convection decreases in mixtures if a constant total pressure is assumed. However, if $p_{\text{mix}}/p_{\text{SF6}}$ is equal to curve p^0 of Fig. 3, for equal dielectric strength the change in total heat transfer is minimal.

In order to confirm this hypothesis, a temperature rise test was carried out in accordance with IEC 60694 on a three phase 145 kV circuit-breaker at a current of 2500 A. The test was performed at an absolute pressure of 4 bar of pure SF_6 gas, then repeated with a mixture of N_2/SF_6 gas (80%/20%) at 7 bar. The maximum deviation observed between the test with pure SF_6 and the test with the gas mixture was only 2,5% of the temperature rise. N_2/SF_6 mixtures and pure SF_6 of equal dielectric strength have similar thermal cooling properties.

9. CONCLUSION

N_2/SF_6 mixtures offer good insulation properties, even at low SF_6 contents. A dielectric strength equivalent to pure SF_6 can be achieved with a moderate pressure increase. However, the arc quenching ability at current zero and the resulting current interruption performance in such mixtures is poor. Even the switching capability of disconnectors for small bus charging currents is considerably degraded, due to the high risk of flashover to ground during arcing between contacts. Altogether, such mixtures can only be applied in HV equipment without switching devices, such as Gas Insulated Lines (GIL). In these applications they offer many advantages. The amount of SF_6 and the SF_6 leakage rate can be considerably reduced compared to pure SF_6. The breakdown voltage in the presence of defects in such mixtures is slightly lower than in pure SF_6 of equal dielectric strength. However, all existing diagnostic systems can be applied with an equivalent or higher detection sensitivity than in pure SF_6. N_2/SF_6 mixtures permit the same power transfer capability for a GIL as pure SF_6 of equal dielectric strength, since they possess equivalent cooling properties.

10. REFERENCES

[1] CIGRE TF D1.03.10: *N_2/SF_6 Mixtures for Gas Insulated Systems*, CIGRE-Report D1-201, Paris, 2004.

[2] CIGRE WG 23.01 TF 02: *Guide for SF_6 Gas Mixtures*, Technical Brochure No 163, 2000.

[3] CIGRE WG 23/21/33.15: *Gas Insulated Transmission Lines*, Technical Brochure 218, 2003.

[4] M. Ermel: *The N2-SF6 Gas Mixtures as Insulating Medium for the High Voltage Technology* (German), ETZ-A, Bd. 96, 1975, pp. 231-235.

[5] N.H. Malik, A.H. Qureshi: *Breakdown Gradients In SF_6-N_2, SF_6-Air and SF_6-CO_2 Mixtures*, IEEE Trans. on Electrical Insulation, Vol. 15, 1980, pp. 413-418.

[6] T.W. Dakin, G. Luxa, G. Oppermann, J. Vigreux, G. Wind, H. Winkelkemper: *Breakdown of Gases in Uniform Fields*, Electra No 32, 1974, pp. 61-82.

[7] W. Boeck, R. Graf, M. Finkel: *Effect of Surface Roughness and Curvature on Streamer Inception and Breakdown of N_2/SF_6 Mixtures*, 7th Int. Conf. on Properties and Applications of Dielectric Materials, Nagoya, 2003, pp. 543-546.

[8] C. Neumann: *N_2 an Economically Acceptable Insulation Medium for Gas Insulated Equipment?* Contribution in Joint Session 21/23/33, Question 1-2, CIGRE, Paris, 1998.

[9] I. Galimberti, N. Wiegart: *Streamer and Leader Formation in SF_6 and SF_6 Mixtures under Positive Impulse Conditions*
I. Corona Development, J.Phys. D: Appl. Phys. 12, 1986, pp. 2351-2361
II. Streamer to Leader Transition, J. Phys. D: Appl. Phys. 13, 1986, pp. 2363-2379.

[10] W. Boeck: *Solution of Essential Problems of Gas Insulated Systems for Substations (GIS) and Lines (GIL)*, 7th Int. Conf. on Properties and Applications of Dielectric Materials, Nagoya, 2003, pp. 1-8.

[11] R. Graf: *Insulation Behaviour of N_2-SF_6 Mixtures for Gas Insulated Apparatus* (German) Fortschritt-Berichte VDI, Reihe 21, ISBN 3-18-333521-2, 2002.

[12] I.W. Mc Allister: *Electric Fields and Electrical Insulation*, IEEE Trans. on Electrical Insulation, Vol. 9, No 5, 2002, pp. 672-696.

[13] A. Pedersen: *The Effect of Surface Roughness on Breakdown in SF_6*, IEEE Trans. on Power Apparatus and Systems, Vol. 94, No 5, 1975, pp. 1749-1753.

[14] A. Diessner, M. Finkel, A. Grund, F. Kynast: *Dielectric Properties of N_2/SF_6 Mixtures for Use in GIS or GIL*, 11th Int. Symp. on High Voltage Engineering, London, 1999, Vol. 3, 3.67.

[15] R. Graf, W. Boeck: *Defect Sensibility of N_2-SF_6 Gas Mixtures with Equal Dielectric Strength*, Annual Report CEIDP 2000, Victoria, Vol. 1, pp. 442-425.

[16] H. Hama, K. Inami, M. Miyashita, M. Yoshimura: *Dielectric Performance of GIB Applying N_2/SF_6 Mixtures under Metallic Particle Contamination*, XIII. Int. Conference on Gas Discharges and their Applications, Glasgow, Vol. 2, 2000, pp. 996-999.

[17] R. Graf, G. Schöffner: *Determination of Inception and Breakdown Voltages of N_2/SF_6 Gas Mixtures in Strong Inhomogeneous Fields*, IX. Int. Symp. on Gaseous Dielectrics, Ellicott City, 2001, pp. 511-516.

[18] CIGRE WG 15.03: *Effects of Particles on GIS Insulation and the Evaluation of Relevant Diagnostic Tools,* CIGRE-Report 15-103, Paris, 1994.

[19] CIGRE Working Group 15.03: *Diagnostic Methods for GIS Insulating Systems*, CIGRE Report 15/23-01, Paris, 1992.

[20] S. Meijer: *Partial Discharge Diagnosis of High-Voltage Gas-Insulated Systems*, Optima Grafische Communicatie Rotterdam, ISBN 90-77017-23-2, 2001.

[21] L.E. Lundgaard, M. Runde, B. Skyberg: *Acoustic diagnosis of SF_6 gas insulated substations: a theoretical and experimental basis*, IEEE Transactions on Power Delivery, Vol. 5, No. 4, 1990, pp. 1751-1759.

[22] H.D. Schlemper, R. Kurrer and K. Feser: *Sensitivity of On-Site Partial Discharge Detection in GIS*, 8th Int. Symp. On High Voltage Engineering, Yokohama, Vol. 3, 1993, pp. 157-160.

[23] B.F. Hampton, R.J. Meats: *Diagnostic Measurements at UHF in Gas Insulated Substations*, IEE Proceedings, Vol. 135, Pt. C, No. 2, 1988, pp. 137-144.

[24] J.S. Pearson, B.F. Hampton, A.G. Sellars: *A continuous UHF Monitor for Gas-Insulated Substations*, IEEE Transactions on Electrical Insulation, Vol. 26, No. 3, 1991, pp. 469-478.

[25] I. Herbst: *PD-Measurement in GIS – A Theoretical and Experimental Comparison of Different Electrical Measurement Techniques*, CIGRE Symposium, Berlin, 1993, 130-02.

[26] A. Bargigia, W. Koltunowicz, A. Pigini: *Detection of Partial Discharges in Gas Insulated Substations*, IEEE Trans. on Power Delivery, Vol. 7, No. 3, 1992, pp. 1239-1249.

[27] L.E. Lundgaard, B. Skyberg, A. Schei, A. Diessner: *Method and Instrumentation for Acoustic Diagnoses of GIS*, CIGRE-Report 15-309, Paris, 2000.

[28] G. Schöffner; W. Boeck: *PD Measurements in N_2-SF_6 Gas Mixtures with the UHF Method*, 11th Int. Symp. on High Voltage Engineering, London, 1999, 5.86.

[29] E. Gulski: *Digital Analysis of Partial Discharges*, IEEE Trans. on Dielectrics and Elecrical Insulation, Vol. 2 No. 5, 1995, pp. 822-837.

[30] S. Meijer, E. Gulski, J.J. Smit, R. Brooks: *Comparison of Conventional and VHF/UHF Partial Discharge Detection Methods for SF_6 Gas Insulated Systems*, 10th Int. Symp. on High Voltage Engineering, Montreal, Vol. 4, 1997, pp. 187-190.

[31] D. Aschenbrenner, H.-G. Kranz: *Diagnosis Potential of Different Partial Discharge Features of Diverse PD Defects in N_2/SF_6 Mixtures*, 7th Int. Conf. on Properties and Applications of Dielectric Materials, Nagoya, 2003, pp. 69-72.

[32] R. Patsch, M. Hoof, C. Reuter: *Pulse-Sequence Analysis, a Promising Diagnostic Tool,* 8th Int. Symp. on High Voltage Engineering, Yokohama, Vol. 4, 1993, pp. 157-160.

[33] A. Girodet: Contribution in Joint Session 21/22/33, Question 2, CIGRE, Paris, 2000.

[34] L. Niemeyer, L. Ullrich, N. Wiegart: *The Mechanism of Leader Breakdown in Electronegative Gases*, IEEE Trans. on Electrical Insulation, Vol. 24, No. 2, 1989, pp. 309-324.

[35] W. Boeck, K. Fröhlich: *GIS Disconnector testing*, 7th Int. Symp. on High Voltage Engineering, Dresden, 1991, No 31.01, pp. 9-12.

[36] J. Lopez-Roldan, T.W. Irwin, S. Nurse, C. Ehden, J. Hannsen: *Design, Simulation and Testing of an EHV Metal-enclosed Disconnector*, 11th Int. Symp. on High Voltage Engineering, London , 1999, Vol. 3, 3.108.

[37] CIGRE Task Force 23.10.01: *SF_6 Recycling Guide – Re-Use of SF_6 Gas in Electrical Power Equipment and Final Disposal.*,
1) Electra No 173, 1997, pp. 43-71
2) Technical Brochure No 117, 1997.

[38] CIGRE WG 23.03: *Handling of SF_6 and its Decomposition Products in Gas Insulated Switchgear*
1st *part*, Electra No 136, 1991, pp. 69-89
2nd part, Electra No 137, 1991, pp. 81-105.

[39] L. Vial, A.M. Casanovas, I. Coll, J. Casanovas: *Decomposition Products from Negative and 50 Hz AC Corona Discharges in Compressed SF_6 and SF_6/N_2 (10:90) Mixtures. Effect of Water Vapour Added to the Gas*, J. Phys. D: Appl. Phys. 32, 1999, pp. 1681-1692.

[40] W.D. Yuan, B. Srigengan, J.W. Spencer, S. Taylor, J. Lopez-Roldan, M. Oliver: *Residual Gas Analysis of SF_6 and N_2-SF_6 Gas Mixtures after Low Current Disconnector Switching*, 13th Int. Conf. on Gas Discharges and their Applications, Glasgow, 2000, pp. 860-863.

[41] I. Coll, A.M. Casanovas, L. Vial, A. Gleizes, J. Casanovas: *Sparking-Induced Decomposition of 10% SF_6–90% N_2 Mixtures: Effect of a Solid Organic Insulator, Oxygen and Water*, J. Phys.D: Appl. Phys. 33, 2000, pp. 1348-1359.

[42] C.G. Henningsen, G Kaul, H. Koch, A. Schuette, R. Plath: *Electrical and Mechanical Long-Time Behavior of Gas-Insulated Transmission Lines*, Cigre Report 21/23/33-03, Paris, 2000.

[43] G. Babusci, E. Colombo, R. Speziali, G. Adrovandi, C. Piazzo, M. Lissandrin, R. Cordioli, R.Bergmann: *Assessment of the Behaviour of Gas-Insulated Electrical Components in the Presence of an Internal Arc*, Cigre Report 21/23/33-03, Paris, 1998.

[44] CIGRE WG 21.12: *Calculation of the Continuous Rating of Single Core, Rigid Type, Compressed Gas Insulated Cables in Still Air with no Solar Radiation*, Electra No 100, 1985, pp. 65-75.

[45] K. Itaka, T. Araki, T. Hara: *Heat Transfer Characteristics for Gas Spacer Cables*, IEEE Trans. on Power Apparatus and Systems, Vol. PAS-97, 1978, No 5, pp. 1579-1585.

[46] J. Vermeer: *A Simple Formula for Calculation of the Convective Heat Transfer between Conductor and Sheath in Compressed Gas Insulated (CGI) Cable*, Electra No 87, 1983, pp.107-113.